Journal of Advanced Joining Processes 9 (2024) 100200

Contents lists available at ScienceDirect

Journal of Advanced Joining Processes

journal homepage: www.sciencedirect.com/journal/journal-of-advanced-joining-processes

Corrosion failures of flanged gasketed joints: A review

Soroosh Hakimian, Abdel-Hakim Bouzid, Lucas A. Hof *

Mechanical Engineering Department, École de technologie supérieure, 1100, rue Notre-Dame Ouest, Montreal, Québec, H3C 1K3, Canada

ARTICLE INFO

Keywords:
Flanged gasketed joints
Pipeline
Corrosion
Marine environment
Materials selection

ABSTRACT

Corrosion-induced leakage in flanged gasketed joints is a critical issue in various industries, with implications for safety, environmental compliance, and economic sustainability. This review paper examines the mechanisms and factors contributing to corrosion-related failures in these joints, clarifying the diverse range of materials, operating conditions, and gasket types that influence their susceptibility to degradation. The paper investigates the key corrosion processes, such as pitting, crevice, and galvanic corrosion, that can initiate and propagate in the joint's critical areas. It explores the role of environmental factors, including microorganisms, temperature, flow, and chlorination, in accelerating the corrosion process. Additionally, the influence of gasket materials and design on corrosion susceptibility is investigated, highlighting the importance of selecting appropriate materials and sealing technologies. Furthermore, it reviews various corrosion monitoring techniques that can help identify corrosion early, ensuring the integrity and reliability of flanged gasketed joints.

Introduction

A bolted flanged joint is a widely employed method for connecting piping systems and pressure vessels that handle fluids at elevated pressures and temperatures. These joints find frequent use in industries such as seawater handling, hydrocarbons, petrochemical and nuclear applications. Their primary advantage lies in the ease of assembly and disassembly, distinguishing them from welded joints (Nechache and Bouzid, 2007). In applications where these joints are used for holding or transferring fluids, there is a risk of metal-to-metal contact between the flanges causing leakage due to surface irregularities. In order to establish a secure and leak-free connection, gaskets made of comparatively softer materials are placed between the mating surfaces of the flanges. Gaskets in flange joints typically have lower stiffness compared to other joint components. They deform easily when subjected to a compressive load, filling in surface irregularities and leakage paths (Nelson et al., 2023). Gaskets play a significant role in preventing leakage in such joints. A schematic illustration of bolted flanged gasketed joints can be seen in Fig. 1. Gaskets must have specific characteristics to be suitable for use. These characteristics include sealability, chemical resistance to the media, and tolerance toward pressure changes, temperature exposure, and creep (Rice and Waterland, 2014; Nurhadiyanto, 2014). The most crucial concern in bolted flanged gasketed joints is the potential leakage of the enclosed fluid (Abid and Nash, 2003; Bouzid, 2009).

Throughout history, numerous accidents involving pipelines have been documented, with a significant portion attributed to fluid leaks during the transportation of substances like water, crude oil, steam, natural gas, and hazardous chemicals to different destinations. The use of pipelines has experienced notable growth over the past two decades, and pipeline accidents have been reported across the globe, with Canada and the United States ranking highest in incident frequency. Some of these incidents have even resulted in explosions, leading to tragic fatalities. Effective pipeline and joint design can play a key role in reducing such incidents (Nelson et al., 2023).

In seawater and hydrocarbon services, bolted flanged joints are susceptible to corrosion, especially at the interface between the gasket and the flange. Detecting corrosion at the flange interface before leakage occurs is also challenging, which can lead to costly consequences (Bond et al., 2018). Remedial or replacement work often results in unscheduled downtime, unplanned costs, and loss of revenue (Kazeminia and Bouzid, 2016). Flange face corrosion is a significant threat to the integrity of bolted flanged gasketed joints and can lead to potentially severe leakage issues. It has been repeatedly observed that bolted flanged joints suffer premature failure due to corrosion, highlighting the necessity for an analysis of the root causes and the development of preventive strategies (Kölblinger et al., 2022; Tavares et al., 2018; Martin et al., 2004; Kain, 1998; Larché et al., 2016; Tsuda et al., 2021). When the flange faces, where the gasket is seated, are exposed to corrosive substances of the transported fluids or to marine environment, they can deteriorate over

* Corresponding author at: Mechanical Engineering Department, École de technologie supérieure, 1100, rue Notre-Dame Ouest, Montreal, Québec, H3C 1K3, Canada.
E-mail address: lucas.hof@etsmtl.ca (L.A. Hof).

https://doi.org/10.1016/j.jajp.2024.100200

Available online 5 February 2024

Nomenclature and Symbols

UNS	Unified Numbering System
RTJ	Ring Type Joint
SCC	Stress Corrosion Cracking
PREN	Pitting Resistance Equivalent Number
PTFE	Polytetrafluoroethylene
RO	Reverse Osmosis
MIC	Microbiologically Induced Corrosion
CPT	Critical Pitting Temperature
CCT	Critical Crevice Temperature
CRA	Corrosion Resistant Alloy
ZRA	Zero Resistance Amperemeter
SS	Stainless Steel
DSS	Duplex Stainless Steel
SDSS	Super Duplex Stainless Steel
EPDM	Ethylene Propylene Diene Monomer
XRD	X-Ray Diffraction
EDX	Energy-dispersive X-ray
FT-IR	Fourier Transform Infrared Spectroscopy
SEM	Scanning Electron Microscope
OCP	Open Circuit Potential

time. Pitting and crevice corrosion damage the quality of the faces of the flanges, compromising the evenness and smoothness required for an effective seal. As the flange faces corrode, they lose their ability to maintain uniform pressure distribution across the gasket, making it difficult to retain fluid pressure (Tavares et al., 2018; Fischer and Zitter, 1960). This corrosion-induced degradation can result in gaps, irregularities, or pitting on the flange face, rendering the gasket sealing task complex and ultimately allowing fluid to leak.

Over the last six decades, extensive research has been conducted on the corrosion of bolted flanged joints. Various studies in the literature have documented instances of premature failures attributed to galvanic (Hu et al., 2020) and crevice corrosion (Kölblinger et al., 2022; Larché et al., 2016; Long et al., 2022; Mathiesen and Bang, 2011) occurring between the gaskets and flange faces. Due to its relatively high corrosion currents, galvanic corrosion accelerates the flange surface corrosion in cases where graphite is used in sheet gaskets, in metallic gaskets, or in semi metallic gaskets (Francis and Byrne, 2007). Gaps or crevices between flanges due to the presence of the gasket are potential locations for crevice corrosion to take place. Flange face corrosion occurs due to fluid penetration through gaps created at the flange-gasket interface. These gaps are created by material loss due to corrosion and aging and facilitated by the loosening of the joint due to the creep-relaxation of the joint (Nechache and Bouzid, 2007; Nechache and Bouzid, 2008; Bouzid et al., 1995), rotation on the flange (Bouzid et al., 1994; Bouzid et al., 2004), and waviness and misalignment (Worden, 2014). The corrosion behavior of the flange is influenced by metallurgical factors, environmental conditions, and the flange and gasket materials (Kain, 1998; Mathiesen and Bang, 2011).

In summary, the corrosion-related failures of flanged gasketed joints can be attributed to a variety of factors. Contributing factors include the flange and gasket material compatibility, the presence of corrosive agents such as O_2, SO_2, and CO_2, stagnant zones, chemical compatibility, temperature, and metallurgical factors. Despite the recurring incidents of flanged gasketed joint failures due to corrosion, there is a lack of predictive rules or methodologies to prevent such failures. Identifying the precise reasons for corrosion-related failures in flanged gasketed joints during operation is a complex task. Therefore, given the frequent occurrence of these failures and the existing literature, there is a significant demand for a comprehensive study on the factors causing these failures, preventative measures, and corrosion inspection techniques,

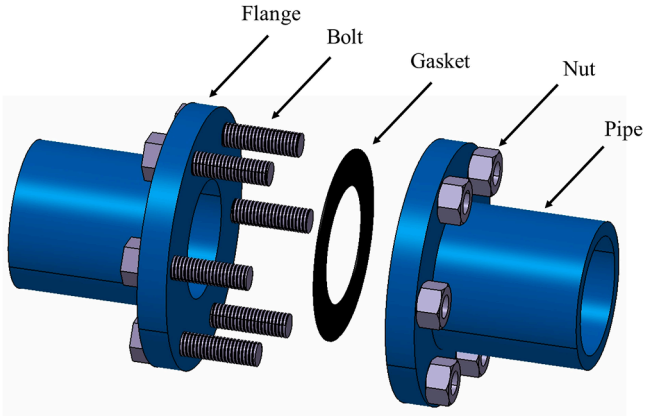

Fig. 1. Schematic of a bolted flanged joint with a gasket placed between two flanges, and tightened by bolts.

with a particular focus on the corrosion occurring on the flange face. The purpose of the work presented in this paper is to explore the failure mechanisms associated with corrosion in flanged gasketed joints, the factors that influence such failures, preventive measures, and techniques for monitoring corrosion.

After introducing the relevance of corrosion failures of flanged gasketed joints in this section, the second section highlights the review methodology, discussing the procedures employed for data collection and literature review. The subsequent section includes an analysis of failure cases and identifies root failure causes, revealing primary corrosion mechanisms and influential factors. Following this failure analysis, the corrosion mechanisms on the flange faces in flanged gasketed joints are explored in the next section, presenting a detailed examination of each mechanism and the corresponding evaluation techniques. Corrosion-contributing factors aligned with the identified failure cases are then introduced in a following section. Then, different corrosion monitoring techniques are discussed, offering an insight into effective monitoring practices. The subsequent section concludes the analysis of flange face corrosion based on collected data and root cause analysis. The discussion section utilizes a diagram to illustrate the contribution of each factor to flange corrosion, drawing upon historical

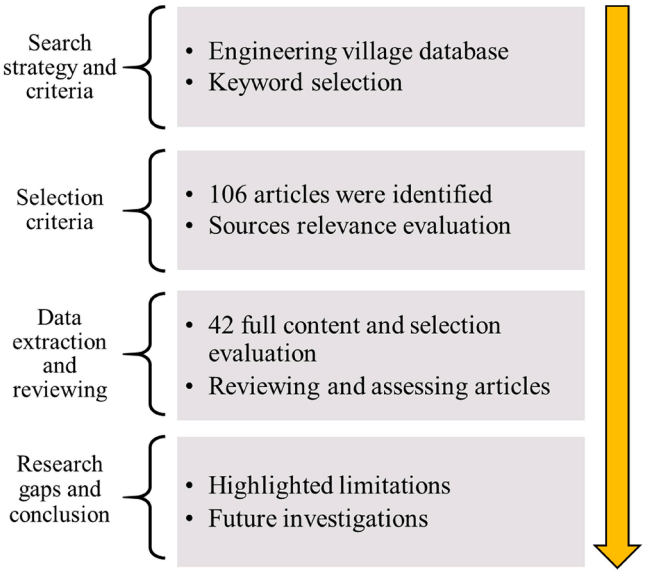

Fig. 2. Flowchart of the deployed review methodology including four steps: search strategy and criteria, selection criteria, data extraction and reviewing, and research gaps and conclusion.

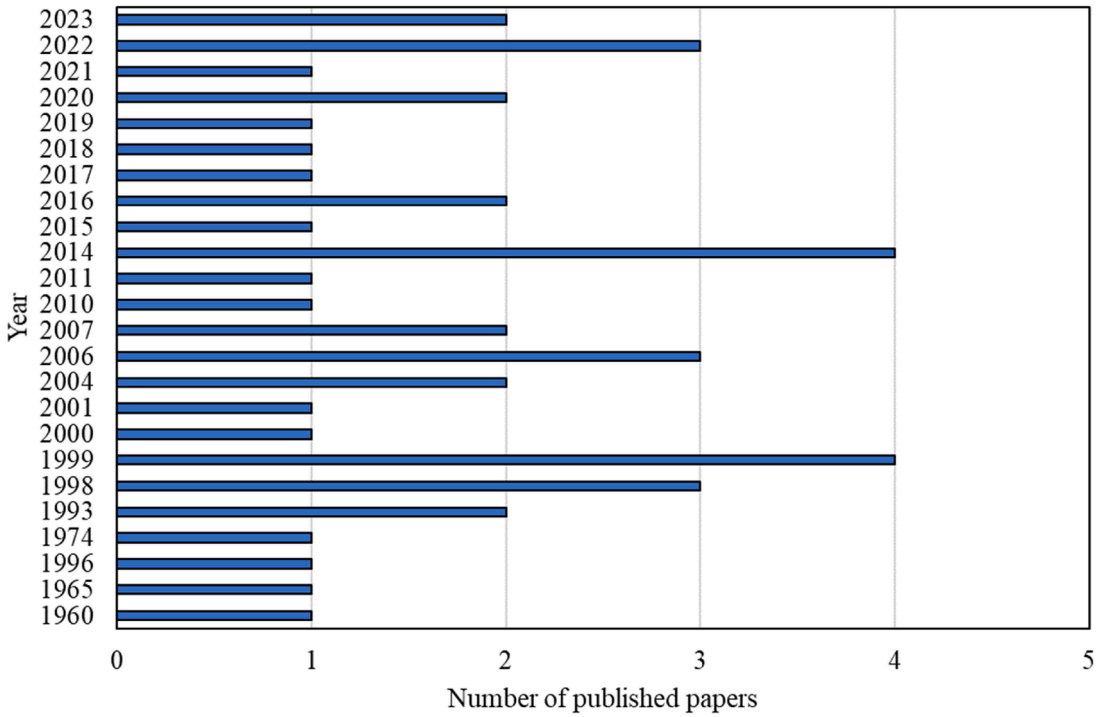

Fig. 3. The number of papers directly studied flange corrosion in bolted flanged joints from 1960 to 2023.

data. Finally, the last section concludes the review study highlighting its most important findings.

Review methodology

The review methodology is structured into four distinct sections, each of which is crucial in guiding the approach and analysis employed in this study. These four sections are outlined in the flowchart presented in Fig. 2, which provides a visual overview of the methodology organization.

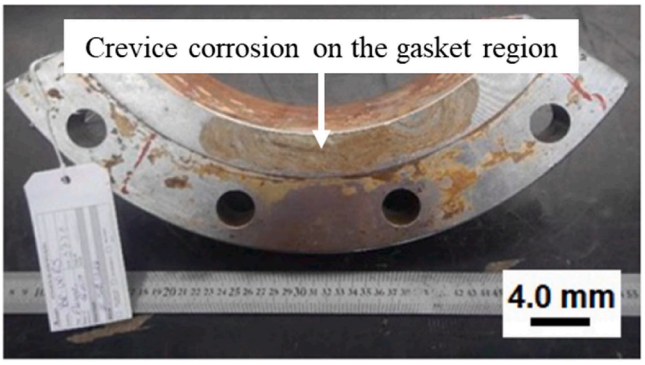

Fig. 4. Crevice corrosion observed on the UNS S32760 SDSS flange face in the gasket region[1] (Kölblinger et al., 2022).

[1] Reprinted from Engineering Failure Analysis, Volume 134, A.P. Kölblinger, S.S.M. Tavares, C.A. Della Rovere, A.R. Pimenta, Failure analysis of a flange of superduplex stainless steel by preferential corrosion of ferrite phase, 2022, with permission from Elsevier.

Search strategy and criteria

The primary method employed to identify relevant literature for this review involved using the Engineering Village search engine, a comprehensive database that predominantly focuses on peer-reviewed journals and conference papers. The keywords used in this review are 'Flange,' 'Gasket,' 'Corrosion,' 'Crevice corrosion,' 'Pitting corrosion,' and 'Galvanic corrosion.' These keywords were selected to explore various aspects of corrosion mechanisms, including crevice, pitting, and galvanic corrosion, as well as the influential factors.

Selection criteria

After conducting a search using the keywords 'Flange,' 'Gasket,' and 'Corrosion,' 106 records directly relevant to corrosion in flanged gasketed joints are identified. However, a large number of records (more than 50,000) are found for other keywords mentioned in the initial search. To ensure relevance and focus on the most recent developments, the most recent papers to clarify corrosion mechanisms, influential factors, and monitoring methods are selected.

Data extraction and reviewing

After the initial selection of relevant papers, a secondary screening process was applied, resulting in 42 articles that primarily focus on flanged gasketed joint corrosion. These 42 articles were thoroughly reviewed and analyzed to form the basis of this review paper. Additionally, 50 articles were included for the analysis of corrosion mechanisms and influential factors.

Research gaps and conclusion

In this step, the research limitations as well as future steps are identified aimed at predicting corrosion in flanged joints and protecting them from it and ultimately preventing leakage. These critical aspects have been included in the concluding section of the review.

Fig. 3 shows the results of the documented literature search, which

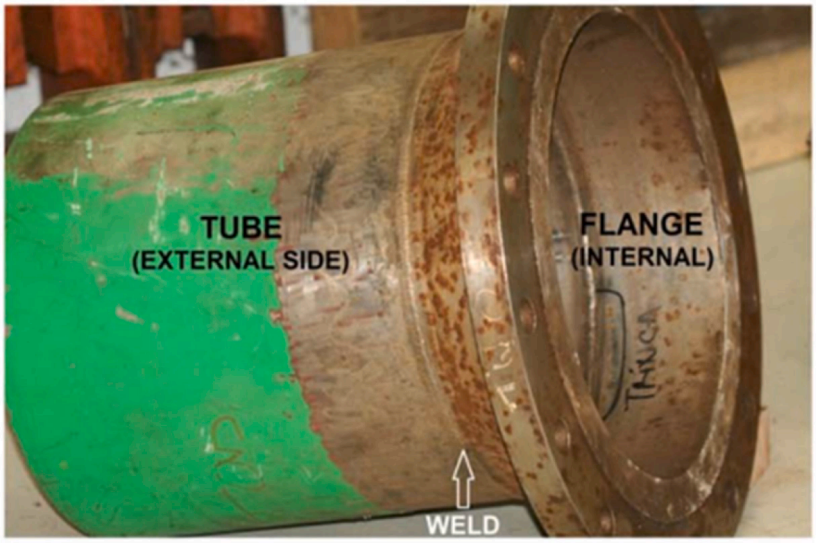

Fig. 5. Flange failure due to severe internal pitting corrosion and circumferential crack, visibly marked by a black line on the internal side of the flange[2] (Tavares et al., 2018).

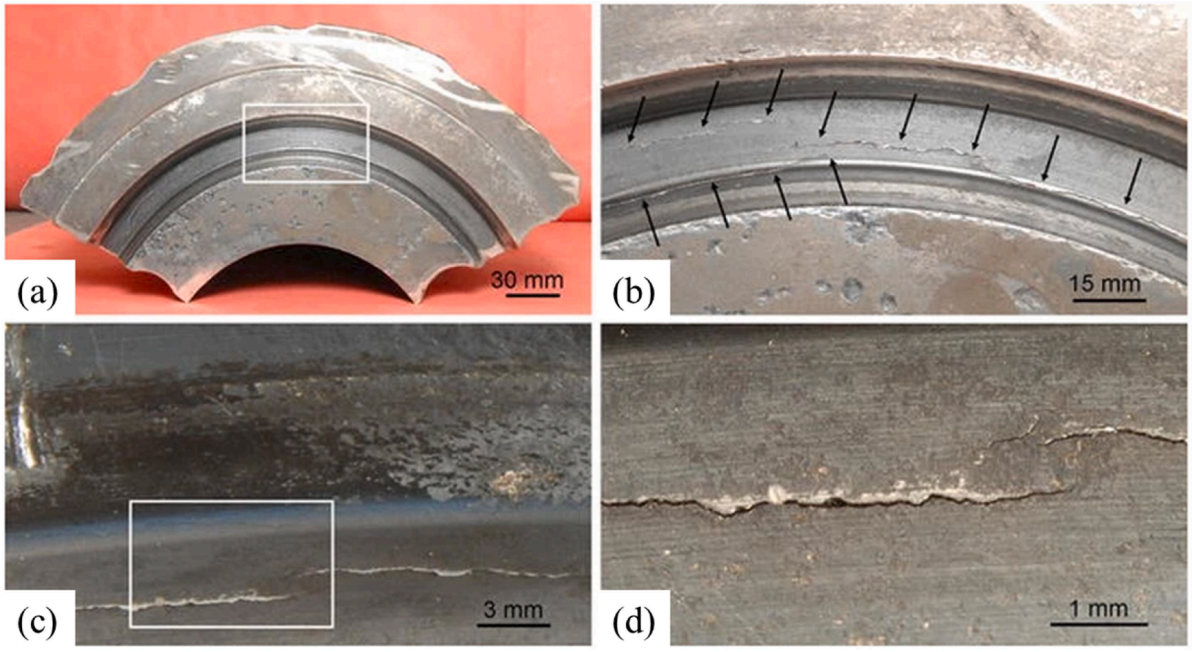

Fig. 6. SCC on the flange RTJ (a) An area of the flange RTJ with a crack, (b) a magnified image (a) where multiple cracks are shown, (c) multiple cracks joining together, and (d) a close-up view of (c)[3] (Gore et al., 2014).

reports that 42 papers directly examined flange and gasket corrosion in bolted flanged joints between 1960 and 2023. Flange failure due to corrosion was the subject of at least one publication every year from 2014 to 2023.

Failure cases

Numerous studies have examined the corrosion of bolted flanged gasketed joints specially over the past sixty years. Different types of premature failures have been reported in the literature due to crevice, pitting, and galvanic corrosions. Mathiessen et al. (2011) reported severe crevice corrosion and subsequent leakages in flange joints within firewater systems on offshore oil and gas production platforms, as well as in chemical plants with bolted flanged connections operating in harsh environments. The affected firewater systems contain stagnant seawater at ambient temperature. The analysis conducted in these studies revealed that UNS31254 stainless steel (SS) flange faces experienced corrosion when used in conjunction with graphite-filled spiral wound gaskets. In another case, crevice corrosion occurred on the face of the

[2] Reprinted from Engineering Failure Analysis, Volume 84, S.S.M. Tavares, J. M. Pardal, B.B. Almeida, M.T. Mendes, J.L.F. Freire, A.C. Vidal, Failure of superduplex stainless steel flange due to inadequate microstructure and fabrication process, 2018, with permission from Elsevier.

[3] Used with permission of Springer Nature BV, from Stress Corrosion Cracking of Ring Type Joint of Reactor Pipeline of a Hydrocracker Unit, Gore, P., Sujata, M. & Bhaumik, S.K, Volume 14, 2014; permission conveyed through Copyright Clearance Center, Inc.

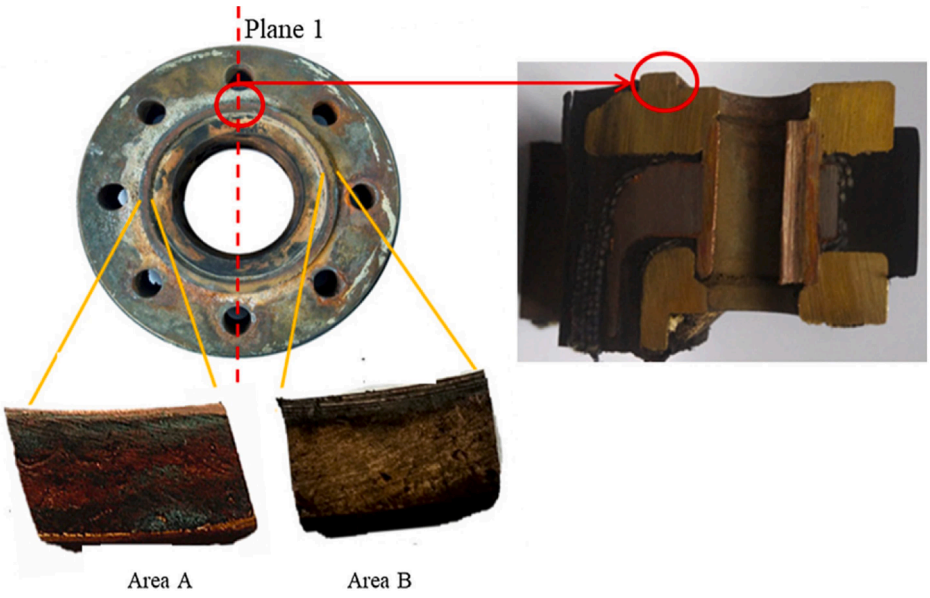

Fig. 7. Corroded surface of a copper flange highlighting two distinct corroded areas labeled A and B. The red dashed line indicates the position of the convex flange's cross section[4] (Hu et al., 2020).

UNS S32760 super duplex stainless steel (SDSS) that was in contact with the gasket (Fig. 4). There has been five years of operation of the flange line, running under a pressure of 1.14 MPa on the top side of an oil platform with seawater at 28 °C on average (Kölblinger et al., 2022). Tavares et al. (2018) reported premature failure of a SS (UNS S32750) flange due to pitting corrosion and cracking (Fig. 5), which was operated with seawater at 40 °C and 0.1 MPa of pressure in a discharge water line of an offshore platform.

Gore et al. (2014) studied the failure of a flange used with ring type joint (RTJ) that was part of the reactor pipeline of a hydrocracker unit. Following a periodic shut-down of the unit, cracks were observed on the flange grooves and RTJ gaskets (Fig. 6). At the time of failure, the hydrocracker had been in service for approximately 11 years. RTJ gaskets were manufactured from stabilized grades of austenitic SS, specifically type 321 and type 347. Further investigations revealed that the RTJ gaskets failed due to trans-granular stress corrosion cracking (SCC). This cracking was initiated by the formation of polythionic acid resulting from the presence of H_2S in the process gas, combined with the presence of H_2O within the system. Based on empirical evidence, it was suggested that the hydrocracker unit was improperly shut down during the last maintenance, which allowed O_2 and H_2O to enter the system.

Tsuda et al. (2021) reported severe corrosion on ASTM A 105 flange surface in a modular plant construction. According to a root cause analysis, the extended construction period during modular construction has resulted in significant corrosion of flange faces due to water ingress into tightly fastened flanges. The modules were transported via sea from fabrication yards to the plant site for assembly. Upon arrival at the plant site, it was observed that the flange faces, including the surfaces in contact with the gaskets, exhibited severe corrosion, despite the flanges having been tightened at the module fabrication yards.

Bengtsson (2015) focused on corrosion of flange faces in a backup diesel cooling system that uses brackish water which caused drips and leaks. It was believed that the graphite gasket used with UNS S31254 SS flanges could cause galvanic corrosion in the presence of brackish water. UNS S31254 SS is a noble material, and the graphite gasket is more noble than UNS S31254 with a potential difference of 0.3 V. The analysis results indicated that several factors contributed to the corrosion acceleration of the SS flange surface. These factors included the presence of a crevice between the flange and gasket, inadequate placement of the weld, and the presence of chlorides in the water. Furthermore, the galvanic current had a synergistic effect on the corrosion of the flange face, leading to increased damage from corrosion.

Hu et al. (2020) investigated a corroded copper flange that caused leakage in a diesel engine cooling system in less than one year of service. A Monel spiral wound gasket filled with PTFE was used with the copper flange. The chemical composition analysis showed that the base material of the flange contained 69.7 % Cu and 28 % Zn. As shown in Fig. 7, the corroded surface of the flange has a red ochre color (area A), and a yellow ochre area (area B). The authors took samples from these two areas and did a chemical analysis. Based on the results, in the red ochre area, the content was 86 % Cu, and 3.61 % Zn, while in the yellow ochre area, the content was 55.27 % Cu and 39.20 % Zn. This indicates that dezincification corrosion occurred more in the area A than area B. Due to the dezincification corrosion, pores are formed on the flange surface, the PTFE coating on the Monel insert is not enough thick to fill in the pores due to the limited deformation; consequently, the fluid leaked through the pores.

In a study by Ji et al. (2023), it was noted that corrosion was identified on the inner wall and sealing groove end face of a surface pipeline flange after a year of operation in a western Chinese oilfield. Failure analyses indicated that the flange's chemical composition and mechanical properties complied with the specified parameters. The primary reason for the corrosion observed was attributed to CO_2-induced corrosion. Furthermore, the elevated temperature and the high flow rate of the medium significantly accelerated the corrosion process. The corrosion of the sealing groove end face, on the other hand, was a result of galvanic corrosion, with the difference in corrosion potential between the flange and gasket being the principal factor driving this phenomenon. The corroded sealing groove of an ASTM A105 carbon steel flange is depicted in Fig. 8(a), while Fig. 8(b) displays a magnified image of the corroded area.

Al-Abbadi et al. (2017) reported corrosion failure of Inconel 625 flange faces were designed for 30 years operation, but failed after two years in the cooling system containing elevated temperature seawater. The investigation determined that the utilization of Inconel gaskets coated with graphite resulted in galvanic corrosion on the flange

[4] Reprinted from Engineering Failure Analysis, Volume 109, Qiangfei Hu, Yuchen Liu, Tao Zhang, Fuhui Wang, Corrosion failure analysis on the copper alloy flange by experimental and numerical simulation, 2020, with permission from Elsevier.

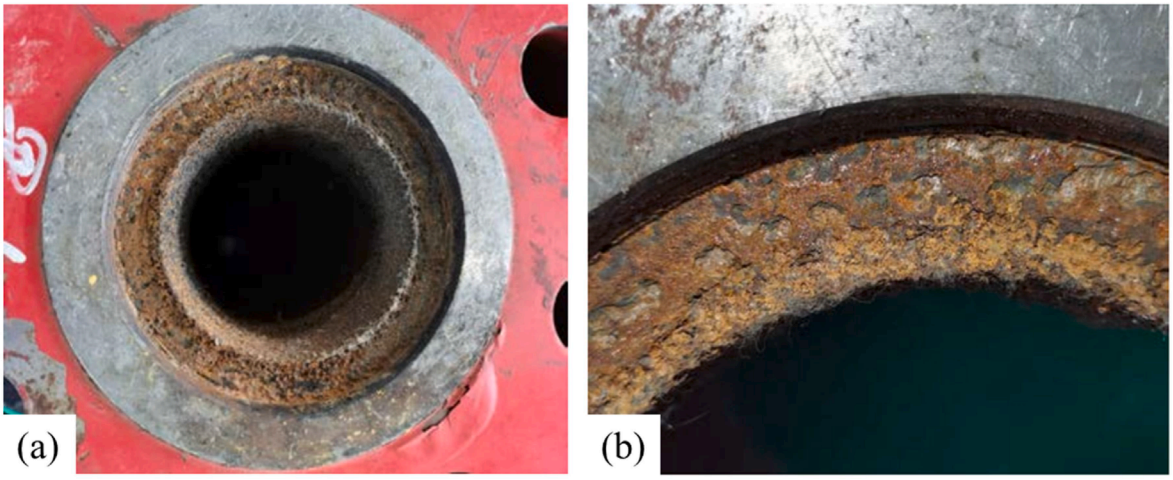

Fig. 8. Macroscopic image of the corroded ASTM A105 flange; (a) corroded sealing groove; (b) magnified corroded sealing groove[5] (Ji et al., 2023).

surfaces in a seawater environment. Consequently, it was advised to substitute the Inconel 625 gaskets coated with PTFE (Polytetrafluoroethylene). Additionally, for the flange surfaces, the recommended course of action was to restore them by applying a weld overlay with the same Inconel 625 metallurgy, and then they were reintroduced into service. Nevertheless, in under two years since the leakage episode, the cooler channel underwent removal from service for a nozzle inspection. The inspection report revealed distinct evidence of pitting at multiple flange surfaces. Notably, this pitting corrosion was exclusively observed in the gasket seating areas of the flange connections, with no signs of corrosion present on any other Inconel 625 surfaces exposed to seawater.

In summary, the cases analyzed in this section have enabled us to identify the specific types of corrosion responsible for flange failures in real applications and the critical factors contributing to the resulting incidents. Refer to Table 1 for a comprehensive overview of the contextual conditions leading to these failures. Subsequently, the following sections of this paper investigate these corrosion types, their underlying mechanisms, the key influencing factors, and the latest monitoring techniques to mitigate and manage these corrosion challenges.

Corrosion mechanisms on the flange faces in flanged gasketed joints

Corrosion is a natural process that occurs when certain materials, particularly metals, react with their environment and undergo deterioration. It is an electrochemical process that involves the gradual degradation and loss of material. For a corrosion reaction to occur, several components are typically involved. These components are essential in creating the necessary electrochemical reactions that drive the corrosion process. The key components are as follows: anode (the site on the metal where oxidation occurs), cathode (the site on the metal where reduction reactions take place), electrolyte (a conducting medium that allows the movement of ions between the anode and cathode), and electron transfer path (for the flow of electrons generated at the anode to the cathode) (Bradford, 2003). These components are all present in bolted flanged gasketed joints.

In the case of bolted flanged joints, the flange serves as the anode, which is the site that will undergo corrosion. The cathode can either be the flange itself or the gasket that is in contact with the flange. The fluid that flows in the pipeline acts as the electrolyte, facilitating the movement of ions between the anode and cathode. The direct contact between the flange and gasket forms the electron transfer path, enabling the flow of electrons from the anode to the cathode. There are different forms of corrosion based on the morphology of the corroded part. However, a few types of corrosion have been observed in bolted flanged joints. According to the literature Table 1, crevice, pitting, and galvanic corrosion do widely occur on the flange faces in bolted flanged joints in industrial installations. The mechanisms of the mentioned types of corrosion will be discussed hereafter.

Crevice corrosion

Crevice corrosion, a common type of corrosion failure in corrosion resistant alloys (CRAs), is regarded as more hazardous than pitting corrosion due to its occurrence in concealed areas that are typically inaccessible and not visible (Costa et al., 2023). This type of corrosion occurs in the crevices, which are wide enough to allow liquid entry but sufficiently narrow to maintain a stagnant zone (Kruger and Begum, 2016). Metals with passive behavior (e.g., SS) suffer more from crevice corrosion because of the passive layer breakdown (Hu et al., 2011). Crevice corrosion primarily occurs in systems containing oxygen, and it becomes more severe when aggressive ions, typically chloride, are present (Luo et al., 2022). This type of corrosion is commonly observed in bolted flanged gasketed joints. The gap within the joint near the gasket area becomes oxygen-depleted and acts as the anodic site. In the presence of seawater, corrosion is exacerbated as negatively charged chloride ions migrate into the crevice. These ions not only counterbalance the accumulation of positive charges around the crevice but also serve as a catalyst, expediting the metal's dissolution. This gradual process leads to the formation of deep pits (Brondel et al., 1994).

Two mechanisms of crevice corrosion are identified in the literature; these are critical crevice solution (CCS) theory and IR drop theory (Kennell et al., 2008; Shojaei et al., 2019). According to the CCS theory, the crevice corrosion mechanism constitutes of two stages; in the first stage, anodic and cathodic reactions occur according to Eqs. (1) and (2), respectively. In Eq. (1), the metal *M* (e.g., iron) is dissolved in aerated seawater and oxygen will be reduced to hydroxide ion, as shown in Eq. (2). Fig. 9 shows a schematic illustrating the components involved in crevice corrosion. These components include the crevice former, responsible for creating a specific crevice gap on the metal surface. Each equation corresponding to the reactions is indicated by numbers in Fig. 9. Number (1) indicates the occurrence of oxidation as per Eq. (1) taking place on the metal surface within the crevice, while number (2) indicates the occurrence of reduction as per Eq. (2) taking place on the

[5] Reprinted from Journal of Physics: Conference Series, Nan Ji, Changliang Li, Peng Wang, Lijuan Zhu, and Chun Feng, Corrosion Cause Analysis of a Surface Pipeline Flange, 2023, CC BY 3.0.

Table 1
Details of corrosion failures of bolted flanged joints.

Gasket material	Flange material	Service period (years)	Type of corrosion	Medium	Root causes	Application	Preventive measures	Ref.
Duplex stainless steel (DSS) spiral wound graphite gaskets	UNS31254 SS flange	1	Crevice	Seawater	- Less resistant duplex grade for the spiral than the flange material - Chlorination of water	A firewater system located on a production platform for offshore oil and gas in the North Sea.	Using polymer gaskets	(Mathiesen and Bang, 2011)
Graphite gaskets	UNS31254 SS flange	–	Crevice and Galvanic	Brackish water	- Existence of a crevice between the gasket and flange - Inadequate positioning of a weld with the presence of chlorides in water - Galvanic currents might have contributed to crevice corrosion along with a synergistic impact	A cooling system to the backup diesels	- Using casted flanges - Using non-conductive gaskets	(Bengtsson, 2015)
Monel alloy gasket in the middle winded by polytetrafluoroethylene (PTFE)	Copper alloy flange	<1	Galvanic and dezincification	Seawater	- Dezincification of the copper flange - Polytetrafluoroethylene on the Monel gasket cannot penetrate into pores formed by dezincification corrosion within copper alloys, so water penetrated to the pores and corrosion occurred	Diesel engine cooling system of a ship	Replacing the using flange with aluminum bronze	(Hu et al., 2020)
Not mentioned	UNS32760 SS flange	5	Crevice	Seawater	- Crevice microbiologically induced corrosion (MIC) occurred on the flange surface	Top side of an oil platform	–	(Kölblinger et al., 2022)
Not mentioned	UNS32760 SS flange	–	Pitting and cracking	Seawater	- Using cast flange instead of forged flange - Chemical composition and microstructure were inadequate for seawater application	A discharge water line of an offshore platform	–	(Tavares et al., 2018)
Ring gasket austenitic SS type 321 and 347	Austenitic SS type 321 and 347	11	Trans granular SCC	H_2S	- The initiation of SCC in RTJ components was attributed to the formation of polythionic acid, which occurred as a result of the presence of H_2S in the process gas and H_2O in the system	Reactor pipeline of a hydrocracker unit	–	(Gore et al., 2014)
Inconel 625 gasket coated with PTFE	Inconel 625 (UNS N06625)	<2	Crevice and pitting	Hydrocar-bon and Seawater	- Susceptibility of Inconel 625 to crevice corrosion when it is used in high-temperature service with high chloride content	Inlet gas cooler	Using alloys with higher CCT, e.g., Hastelloy C-276 instead of Inconel 625	(Al-Abbadi et al., 2017)
304 SS	ASTM A105	1	Galvanic corrosion and erosion	CO_2	- Galvanic corrosion resulting from the contact between the gasket and the flange material The fluid's average flow velocity within the pipeline exceeded the critical erosion velocity. Consequently, the fluid flow inside the pipeline caused erosion to the inner wall of the flange	Oilfield production well	–	(Ji et al., 2023)
-	UNS S42000 martensitic SS	~ 2	Pitting and crack propagation from the pit along the delta ferrite/ martensite interfaces	CO_2	- The presence of chromium-rich carbides within the structure diminished the resistance against pitting corrosion. - Delta ferrite component weakened the crack resistance - The stress level within the sealing structure of the flange played a significant role in influencing the behavior of crack propagation	Ultra deep high-pressure and high-temperature gas well	Optimizing the forging process to reduce the delta ferrite content	(Long et al., 2022)
Corrugated metallic 304 SS	304SS	<1	Pitting corrosion on the gasket	Demineralized water	- Contamination of the water by chloride ions, and excessive compressive preload	Hydrocarbon transfer pipeline in polyethylene plant and piping system	–	(Tawancy, 2019)

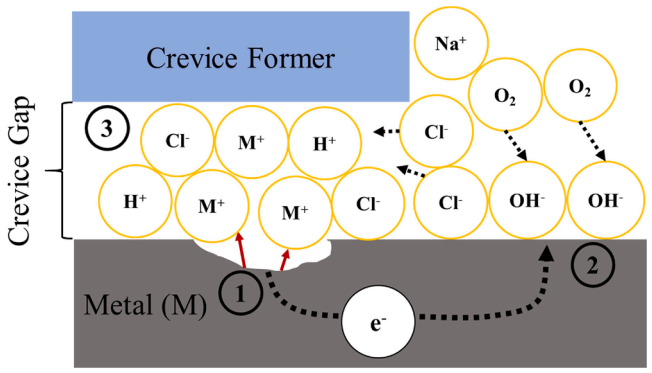

Fig. 9. Illustration of the crevice corrosion, depicting oxygen depletion and acid formation within the crevice in three steps according to CCS theory: 1- the metal (M) is oxidized to (M^+), 2- oxygen (O_2) is reduced to hydroxide ion (OH^-), 3- the metal chloride (MCl) hydrolysis in seawater and forms metal hydroxide (MOH), hydrogen ions (H^+), and chloride ions (Cl^-).

metal surface outside the crevice.

$$\text{Oxidation}: \ M \rightarrow M^+ + e \tag{1}$$

$$\text{Reduction}: \ O_2 + 2H_2O + 4e \rightarrow 4OH^- \tag{2}$$

In the second stage, oxygen concentration decreases over time since species exchange is restricted in the crevice. According to Fig. 9, the absence of oxygen in the crevice gap causes chloride ions to move to the crevice (shown by arrows on the Cl^- ion) to react with an excess positive charge of M^+ and balance the electric charge. Afterwards, the metal chloride (MCl) hydrolysis in water (as stated by Eq. (3)) reacts to give undissolved metal hydroxide and acid. In Fig. 9, number (3) indicates that the reaction as per Eq. (3) taking place within the crevice. Raising the concentration of hydrogen ions and chloride ions accelerates the corrosion rate of metal; furthermore, the higher corrosion rate provides more M^+ ions, and consequently, the amount of acid increases, so this process is autocatalytic. In cases where a passive layer forms on the metal surface, high H^+ and Cl^-concentrations damage the passive layer and drastically increase the corrosion rate. Crevice corrosion is a localized corrosion, since during the time that the metal is being corroded aggressively, the reduction reaction constantly occurs on the exterior surface, so the outer surface of the crevice is protected (Costa et al., 2023) .

$$MCl + H_2O \rightarrow MOH + H^+ + Cl^- \tag{3}$$

In IR drop theory, I refers to the current and R refers to the resistance (Pickering, 1989). According to the IR-drop theory, several factors, including the crevice's geometry, composition, and concentration gradients, contribute to the establishment of a potential difference between the crevice and its surrounding environment. This potential difference, driven by the resistance to electric current flow in the crevice, is known as the IR drop (Kelly and Lee, 2018). In areas where the electric potential decreases to a critical level, denoted as critical potential (E_{crit}), the current density experiences a significant surge. This occurs because the protective passive film loses its stability, causing a shift to active dissolution. The IR-drop mechanism has been gaining attention because it offers insights into corrosion mechanisms in environments containing chloride and those without it, a capability not shared by the CCS model. However, it is important to note that the IR drop model is particularly suitable for metal/electrolyte systems that exhibit both active and passive behavior within the crevice solution (Betts and Boulton, 1993).

Crevice corrosion evaluation involves a range of techniques designed to assess the susceptibility and severity of this localized form of corrosion. These techniques can be broadly categorized into three groups: non-electrochemical or immersion methods, electrochemical methods at open circuit potential, and electrochemical methods with applied signals (Kelly and Lee, 2018; Oldfield, 1987). Table 2 illustrates techniques that are used to evaluate localized corrosion.

Pitting corrosion

Pitting corrosion, which shares similar mechanisms with crevice corrosion, represents another form of localized corrosion. In both of these corrosion types, a distinct alteration in the local environment is a prerequisite for significant damage to occur. The onset of crevice corrosion is marked by the formation of pits within enclosed areas. The primary differentiation between crevice corrosion and pitting corrosion lies in the fact that crevice corrosion necessitates the presence of a physically confined space for initiation. Pitting corrosion, on the other hand, can manifest on exposed surfaces, although some studies have suggested that pitting may also commence at the interface between an inclusion and the matrix (Guo et al., 2021). Pitting corrosion is characterized as an autocatalytic reaction, wherein the dissolved metal converts into metal ions, creating a highly acidic environment that accelerates the local corrosion rate and deepens the pits. In the context of bolted flanged joints, pitting corrosion has been observed predominantly on the inner side (as depicted in Fig. 10) and on flange faces (Tavares et al., 2018; Al-Abbadi et al., 2017). The pitting corrosion resistance can be evaluated using electrochemical methods. The pitting potential (E_{pit}) and the re-passivation potential (E_{rep}) of alloys in different environments are obtained by cyclic potentiodynamic polarization measurements based on the ASTM G61 standard test method. Another standard test method, ASTM G150 (ASTM G192-08(2020)e1 2018), introduces a procedure for obtaining the critical pitting temperature (CPT). This CPT is the highest temperature below which pitting corrosion does not occur. As such, a high material CPT value indicates a good pitting resistance compared to materials possessing lower CPT values.

Galvanic corrosion

When two dissimilar metals are in contact with each other and immersed in a corrosive solution, the metal having a higher potential behaves as a cathode, and the other metal acts as an anode, resulting in the flow of electrons between them (Hack, 2016). Galvanic corrosion, due to its relatively high corrosion currents, could accelerate the flange surface corrosion in cases where graphite containing gaskets are used in combination with flanges (Francis and Byrne, 2007). Graphite exhibits a high level of nobility compared to most metals when exposed to seawater (Francis, 1994). Consequently, it has the potential to induce corrosion, even in the case of high-alloy materials, particularly within crevices. Sheet-type gaskets, such as flexible graphite, are frequently employed in situations involving smaller diameters, low pressures, or lower temperatures. However, as the diameter, pressure, or temperature rises, sheet gaskets become less appropriate due to the heightened risk of blowout. In such cases, semi metallic or metallic gaskets are employed as a solution (Bouzid and Das, 2023). Bengtsson (2015) reported flange face corrosion in brackish water inside a cooling system of backup diesel generators. The flange material used in this system was UNS31254 SS, and a graphite-containing gasket was used to seal the joint. The high potential difference between the gasket and flange material accelerated the crevice corrosion on the flange surface, as is illustrated in Fig. 11.

Ji et al. (2023) conducted an analysis of the corrosion issue observed in a pipeline flange that exhibited corrosion on the inner wall and sealing groove end face after one year of service. The study findings revealed that the main cause of flange face corrosion was galvanic corrosion resulting from the contact between the gasket (made of 304 SS) and the flange material, which had different materials and a potential difference of 0.67 V. Galvanic corrosion depends not just on the potential difference but also critically on the polarization behavior. Therefore, graphite and an alloy that has a passive behavior (e.g., Alloy C-276) may exhibit a significant difference, but the corrosion rate may

Table 2
Techniques to quantify localized corrosion.

Technique	Description	Alloy	Electrolyte	Temperature	Time	Results	Limitations	Ref.
Non-electrochemical or immersion methods	ASTM G48 standard test method	SSs and related alloys	Methods A and B: 6 wt.% ferric chloride ($FeCl_3$) Methods C, D, E, and F: 6 wt. % ferric chloride ($FeCl_3$) + 1% HCl	Methods A and B: 22 °C or 50 °C Methods C, D, E, and F: between 0 °C and 85 °C	Methods A, B, and C: 72h	Mass-loss, maximum penetration depth, attack area, critical crevice temperature (CCT), critical pitting temperature (CPT)	The test methods and their acceptance criteria differ among various oil companies, and each of the outlined methods involves leaving certain details to the test laboratory. These details could have a crucial influence on the final result (Mathiesen and Andersen, 2014).	(ASTM G48-11 (2020)e1 2020)
	ASTM G78 standard test method	Iron-base, Nickel-base stainless alloys	Seawater	Ambient	At least 30 days	Mass-loss, maximum penetration depth, attack area	–	(ASTM G78 - 20 2021)
Electrochemical methods at open circuit	Monitoring open circuit potential	–	–	–	–	Corrosion potential (E_{corr}), initiation of crevice corrosion	Open-circuit measurements cannot provide any data on reaction rate because there is no current flow between the crevice and the reference electrode	(Kelly and Lee, 2018)
	ASTM G71 standard test method	–	–	–	–	Current flow between anode (creviced) and cathode (non-creviced) using ZRA method	This method must be supplemented by weight loss or other techniques, as ZRA only measures net current.	(ASTM G71-81 (2019) 2019)
Electrochemical methods with applied signal	ASTM G61-Cyclic potentiodynamic polarization	Iron-, Nickel-, or Cobalt-based alloys	Appropriate electrolyte that simulates the expected service environment	The temperature should represent the service environment	–	Pitting or crevice potential (E_{pit}, E_{crev}), re-passivation potential (E_{rep}), corrosion potential (E_{corr}), passive current density (i_{pass})	E_{rep} are not highly reproducible particularly when the alloy is not very susceptible to crevice corrosion or when the environment is not highly aggressive.	(ASTM G61 - 86 (2018) 2021; Esmailzadeh et al., 2018; Sridhar and Cragnolino, 1993)
	Potentiostatic test	–	–	–	–	Current vs. time curve provides information about crevice corrosion initiation time and propagation	This method may produce cathodic currents exceeding what a local cathode could provide. Consequently, reaction rates are frequently overestimated when compared to open circuit exposures limited by either anodic or cathodic reactions.	(Kelly and Lee, 2018)
	ASTM G192-standard test method	Corrosion-resistant alloys	Any electrolyte Standard: 1 M NaCl	90 °C or lower	–	Crevice re-passivation potential	This technique tends to be slow and requires a significant amount of time due to the typical occurrence of E_{rep} at low potentials.	(ASTM G192-08 (2020)e1 2020)

not be significant.

The ASTM G71 standard method proposes another method for conducting and evaluating galvanic corrosion tests in different electrolytes (ASTM G71-81(2019) 2019). The galvanic current is measured with a "zero resistance" amperemeter (ZRA), practically having a very low resistance. Such instrument measures the current between two electrodes by short-circuiting them. Fig. 12 presents a schematic illustration of a galvanic current measurement by using electrodes (anode and cathode) partially immersed in an electrolyte and short-circuited by a ZRA. Typically, a coating is applied on both electrodes to ensure a well-defined electrode surface area exposed to the electrolyte. It should be noted that ZRA measurements of galvanic corrosion must be supplemented by weight loss or other techniques because ZRA only measures net current. It does not specify whether the cathode also corrode at a high rate. This can be a problem for some alloys that exhibit a significant active-passive peak, where ZRA measurements can indicate a small galvanic current, but they corrode at a rapid rate (Okonkwo et al., 2021).

In this section, the mechanisms of corrosion types that commonly occur in bolted flanged joints are introduced, along with widely known test techniques. However, it is important to consider the limitations of these methods when evaluating crevice corrosion, pitting corrosion, or

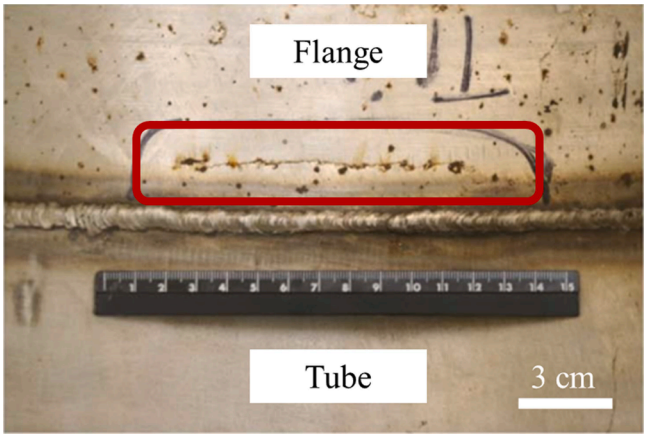

Fig. 10. Severe pitting corrosion observed on the internal side of the SDSS flange near the flange and tube connection, highlighted by the red rectangle[6] (adapted from Tavares et al., 2018).

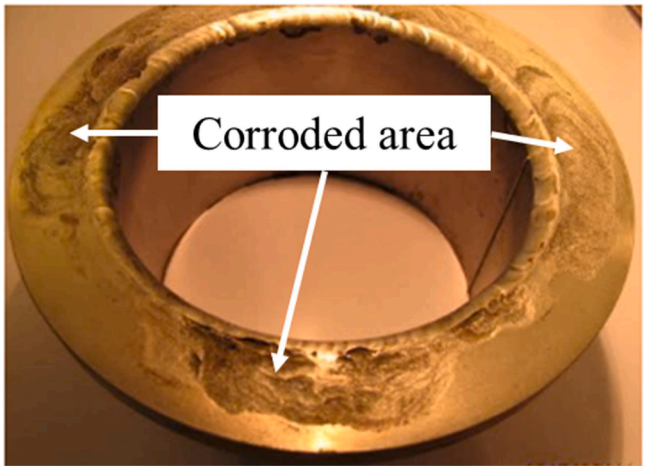

Fig. 11. Crevice corrosion (locations indicated by the arrows) on the face of a UNS31254 SS flange[7] (adapted from Bengtsson, 2015).

galvanic corrosion in bolted flanged joints. Standards such as ASTM G71, G78, and G150 provide standardized test methods with simplified geometric configurations that may not fully represent the complex geometries and conditions encountered in the actual complex structures such as bolted flanged joints. Consequently, the test results may not accurately reflect the actual corrosion behavior in practical applications. Furthermore, these standards do not encompass the wide range of environmental conditions that bolted flanged joints can be exposed to. Factors such as varying temperatures, different corrosive media, and fluctuating exposure durations may not be adequately captured in the testing protocols, limiting the applicability and representativeness of the results. It is important to note that these ASTM standards primarily focus on corrosion evaluation and do not incorporate mechanical loading or stress conditions present in operational bolted flanged joints. The absence of mechanical loading may result in an incomplete understanding of the overall corrosion behavior of the joint under realistic

[6] Reprinted from Engineering Failure Analysis, Volume 84, S.S.M. Tavares, J. M. Pardal, B.B. Almeida, M.T. Mendes, J.L.F. Freire, A.C. Vidal, Failure of superduplex stainless steel flange due to inadequate microstructure and fabrication process, 2018, with permission from Elsevier.

[7] Reprinted from master program thesis, Martin Bengtsson, Investigation of Galvanic Corrosion between Graphite Gaskets and Stainless Steel Flanges, with permission from the author.

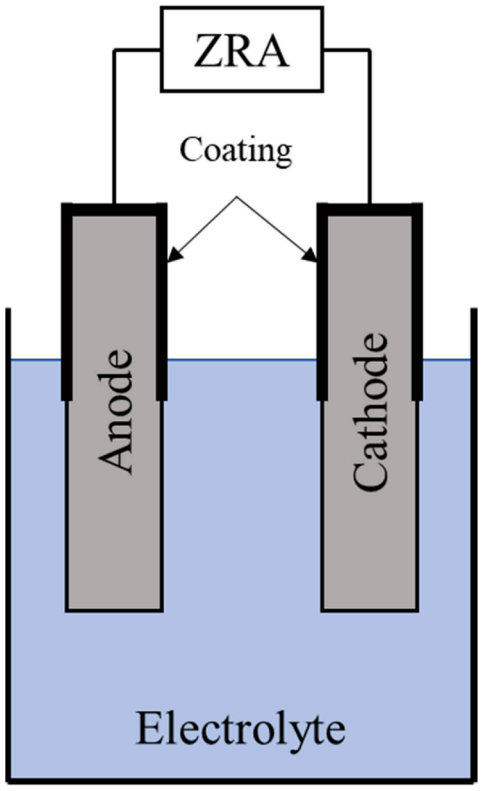

Fig. 12. Schematic of the galvanic corrosion test setup to measure the galvanic current between a partially coated anode and cathode, connected to each other by a zero resistance amperemeter (ZRA) and immersed in an electrolyte.

Table 3
Materials frequently used in flange fabrication.

Name	Grade	Specification
Carbon steel	ASTM A105 (ASTM A105 /A105M - 18 2020), ASTM A350 (ASTM A350 /A350M - 18 2020)	Carbon steel forgings for piping applications
Low alloy steels	ASTM A182 (ASTM A182 /A182M - 20 2020)	Forged or rolled alloy and SS pipe flanges
Stainless steels	ASTM A182	Forged or rolled alloy and SS pipe flanges
Nickel alloys	ASTM B462 (Standard Specification for Forged or Rolled Nickel Alloy Pipe Flanges, Forged Fittings, and Valves and Parts for Corrosive High-Temperature Service n.d 2022)	Forged or rolled nickel alloy pipe flanges, forged fittings, and valves and parts for corrosive high-temperature service

working conditions. For instance, the mechanical loading affects the thickness of the gasket in the joint which determines the size of the crevice and has a strong relationship with the initiation and development of crevice corrosion (Luo et al., 2022; Shojaei et al., 2019). In recent years, researchers have been working on the development of fixtures for measuring flange face corrosion under conditions that closely mimic actual working conditions (Hakimian et al., 2022; 2023).

Corrosion contributing factors

Analysis of corrosion-related failures in the literature reveals that certain factors can accelerate corrosion in bolted flanged joints. This section presents the most critical factors, drawing upon failure analysis and technical research.

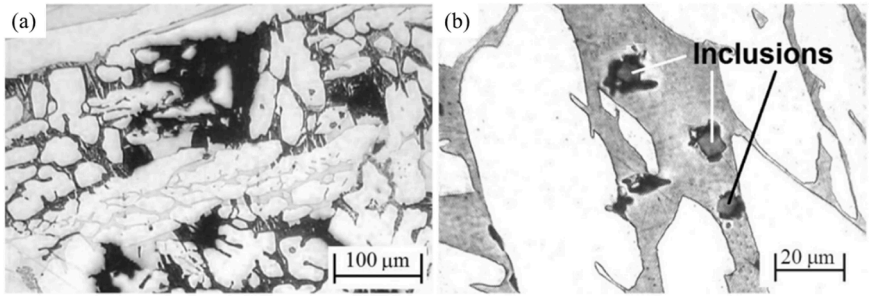

Fig. 13. Observation of pitting after polarization testing (a) region of the high density of σ phase (b) pit nucleation in non-metallic phase[8] (Tavares et al., 2018).

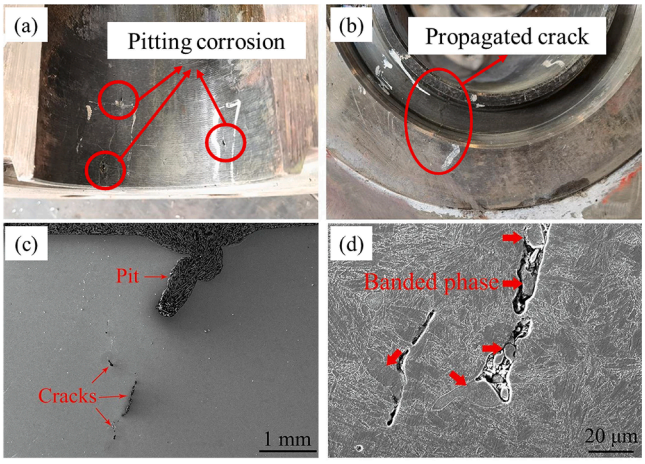

Fig. 14. Corrosion and propagation of cracks on the surface of the pipe flange can be observed as follows: (a) pitting corrosion occurring near the flange end on the inner surface; (b) crack propagation originating from the pit located in the ring groove; (c) the detailed cross-sectional morphology of the region affected by pitting and cracking; (d) a closer examination at a higher magnification[9] (adapted from Long et al., 2022).

Flange material and microstructure

Material selection is one of the most important steps in designing industrial structures (Hakimian et al., 2023). Flanges are manufactured using a variety of materials, including carbon steels, low alloy steels, SSs, and nickel-based alloys. Table 3 provides a list of the most commonly used flange materials, chosen according to the necessary mechanical properties and operational considerations, such as temperature, pressure, and pH, in bolted flanged gasketed systems. Nadarajah's (2004) study focuses on determining the maximum level of corrosion that a weld neck flange face could withstand without compromising its structural integrity, ensuring its suitability for service. The investigation involves a parametric analysis using the finite element method, which encompasses all weld neck flanges specified in the ASME B16.5 Code for Pipe Flanges and Flanged Fittings. This analysis results in the creation of several tables that set limits on corrosion for different classes and sizes of flanges. It is important to note that this research specifically considers

Table 4
Crevice corrosion initiation time (t_{init}) for Ni-Cr-Mo alloys in 65 °C seawater (Martin et al., 2004).

Alloy	PREN	t_{init} (hr)
625	51	2.9
276	73	9.5
59	74	16
2000	76	20
686	77	>120

the A105, A182 Cl 70, and A350 LF2 flange materials and addresses general corrosion on the flange face, taking into account a maximum temperature of 38 °C. It is worth mentioning that although general corrosion can affect carbon steels like A105, the most problematic form of corrosion for flange faces is crevice or pitting corrosion, which spreads rapidly within a localized area.

While there are standard specifications for flange chemical compositions and manufacturing processes, corrosion failures are sometimes observed as a result of discrepancies with the standards. SS flanges used in the oil and gas sector are typically required to be manufactured through forging, as per the ASTM A 182 standard. Nevertheless, it is common to encounter cast flanges on offshore oil and gas platforms, and these cast flanges frequently experience failures within a short timeframe, often within hours or days of being put into service (Kölblinger et al., 2022). Laboratory experiments have demonstrated that crevice corrosion propagates more significantly in cast SDSSs than in wrought SDSSs in seawater ranging from 15 °C to 40 °C (Larché and Dézerville, 2012). In a specific case documented by Tavares et al. (2018), a cast flange was supplied with significant amounts of sigma phase, likely due to the absence of a proper solution treatment. Consequently, the flange failed due to brittleness and pitting corrosion. Following a polarization test, optical microscopy and scanning electron microscopy (SEM) were employed to analyze the material. The analysis revealed that pits nucleated within intermetallic phases and non-metallic inclusions. Fig. 13(a) and (b) depict the existence of non-metallic inclusions within the flange material structure, leading to the formation of intermetallic phases. These inclusions and intermetallic phases serve as preferential sites for pit nucleation, consequently reducing the pitting corrosion resistance of the flange material.

In a study conducted by Long et al. (2022), it was observed that UNS S42000 SS(13Cr) pipe flange exhibited leakage after being in service for 23 months in an ultra-deep high-pressure and high-temperature gas well. This leakage was attributed to pitting corrosion on the inner wall of the flange, leading to the propagation of a crack towards the ring groove. The corresponding illustrations, Fig. 14(a) and (b), depict this situation. Additionally, Fig. 14(c) shows the cross-sectional appearance of the pitting and cracking area near the flange end, while Fig. 14(d) shows that the crack propagated alongside the banded phase. The banded phase is known as delta ferrite, which forms during the forging process at higher temperatures than the austenitizing temperature. The presence of this delta ferrite proved to be a significant factor in the failure of the

[8] Reprinted from Engineering Failure Analysis, Volume 84, S.S.M. Tavares, J. M. Pardal, B.B. Almeida, M.T. Mendes, J.L.F. Freire, A.C. Vidal, Failure of superduplex stainless steel flange due to inadequate microstructure and fabrication process, 2018, with permission from Elsevier.

[9] Reprinted from Engineering Failure Analysis, Volume 142, Yan Long, Jinheng Luo, Ming Yue, Gang Wu, Mifeng Zhao, Nan Ji, Wenwen Song, Qiang Jin, Xianren Kuang, Yujie Fan, Investigation on leakage cause of 13Cr pipe flange used for a Christmas tree in a high-pressure and high-temperature gas well, 2022, with permission from Elsevier.

Table 5
Chemical composition of the materials used as a flange material in the literature.

Material	UNS No.	Other designations	Cr	Ni	Mo	N	Other	PREN	Type	Corrosion failure reported
Stainless steels	S32750	2507	24–26	6–8	3–5	0.24–0.32	Cu <0.5	38–47	Super duplex	Yes
	S42000	420	12–14	<0.5	<0.5	–	Cu <0.5	–	Martensitic	Yes
	S31254	254 SMO	19.5–20.5	17.5–18.5	6–6.5	0.18–0.22	Cu 0.5–1	42–45	Super austenitic	Yes
	S31266	B66	23–25	21–24	5.2–6.2	0.35–0.6	Cu 1–2.5 W 1.5–2.5	46–54	Super austenitic	No
	N08367	Al6XN	20–22	23.5–25.5	6–7	0.18–0.25	Cu 0.75	43–49	Super austenitic	Yes
	S32205	–	22–23	4.5–6.5	3–3.5	0.14–0.2	–	34–38	Duplex	Yes
Nickel alloys	N06625	Inconel alloy 625	20–23	>58	8–10	–	–	40.2–41.3	–	Yes
	N06022	Hastelloy alloy C-22	20–22.5	>58	12.5–14.5	–	W 2.8–3.2	45.5–45.7	–	No
	N06686	Inconel alloy 686	20–23	>58	15–17	–	3–4.4	47–55.1	–	No

system. The presence of a significant amount of delta ferrite promoted the formation of chromium-rich carbides, leading to a decrease in pitting resistance. Additionally, the delta ferrite compromised crack resistance, causing cracks to form along the interfaces of delta ferrite and martensite.

SSs in seawater are highly vulnerable to crevice and pitting corrosion originating from the presence of gaps and crevices in bolted flanged joints (Francis and Byrne, 2007). In order to mitigate degradation by these corrosion types, it is recommended to use SSs with a Pitting Resistance Equivalent Number (*PREN*) higher than 40 to reduce the probability of crevice and pitting corrosion. This *PREN* is defined by Eq. (4), and involves chromium, molybdenum, and nitrogen weight percentages, as these elements stabilize the passive film on SS surfaces (Kang and Lee, 2013; Westin and Hertzman, 2014).

$$PREN = \%Cr + 3.3 \times \%Mo + 16 \times \%N \quad (4)$$

For example, UNS S32750, UNS S31254, and UNS S31266 are high-grade SSs with a *PREN* greater than 40 (Larché et al., 2016) and typically suggested as flange material in corrosive environments. Rogne et al. (1998) used the ASTM G48 test method to compare the crevice corrosion properties of weld overlays of Ni-based alloys to UNS S31254 SSs for seawater applications. Their investigations showed that only alloy 59 is beneficial for use with respect to crevice corrosion initiation compared to UNS S31254 SSs, while all alloys C-22, C-276, 625, and C-4 weld overlays have lower critical crevice temperature (CCT) than the UNS S31254 base material. Martin et al. (2004) ranked the corrosion susceptibility of Ni-Cr-Mo alloys in elevated temperature seawater in combination with gaskets. In their study, a potentiostat controlled the potential at a constant value of 0.3 $V_{Ag/AgCl}$, and the solution temperature was kept constant at 65 °C. As shown in Table 4, it was found that alloy 625, which had the lowest *PREN* among the studied alloys, exhibited crevice corrosion initiation at a lower exposure time (t_{init} = 2.9 h).

Al-Abbadi et al. (2017) investigated the crevice corrosion failure of alloy 625 flange in seawater service at an elevated temperature and proposed an alternative in alloy 686 with a CCT of up to 85 °C. Larché et al. (2016) studied the crevice corrosion performance of several SS and nickel alloys at various temperatures in both natural seawater and chlorinated seawater. In their tests, flanged joints were immersed in seawater for three months, including natural seawater at 30 °C, chlorinated seawater at 30 °C, and chlorinated seawater at 50 °C. They reported that among the tested alloys, flanges made of UNS N06022 and UNS S31266 exhibited resistance to crevice corrosion.

Even high *PREN* SSs are susceptible to crevice corrosion in seawater. Indeed, the *PREN* does not consider significant factors that affect corrosion resistance (e.g., metallurgy, product form, service conditions, geometrical configuration of the confined zones, and etc.); for example, cast alloys have less resistance to crevice corrosion than wrought alloys because of more heterogeneous metallurgical composition (Larché et al., 2016; Larché and Dézerville, 2012). In addition, the validity of *PREN* as a universal method has been questioned in a number of papers (Sridhar, 2022).

Table 6
Crevice corrosion initiation and propagation on 316 SS flange in combination with various gaskets (Kain, 1998).

Gasket material	No. of flanges attacked	Maximum depth (mm)
Fluoroelastomer	0/2	0.00
Red rubber	1/2	0.01
Carbon Fiber + Nitrile	2/2	0.77
Aramid Fiber + Nitrile	2/2	2.1
PTFE	2/2	1.05
Glass Filled PTFE	1/2	1.4
Graphite/SS	1/2	0.69

Although high-grade SSs with a high *PREN* value were used in aggressive environments, other factors, including metallurgical and environmental factors, caused the failure of the flanges. The *PREN* does not consider the negative influence of impurities, such as sulfur and carbon or the effect of microstructure. In fact, it is possible for DSS, and SDSS to have drastically reduced corrosion resistance if the microstructure consists of small amounts of deleterious phases (such as sigma phases) (Fargas et al., 2009). Table 5 summarizes the chemical composition of CRAs that are used in the literature as a flange material.

Gasket material

In bolted flanged joints, the gasket acts as a crevice former; therefore, the gasket material or the type of gasket affects the crevice corrosion on the flange surface. The primary purpose of a gasket in a flanged joint is to prevent leakage from the connection. However, many factors need to be considered in selecting the appropriate type of gasket, including the bolting, the media inside the pipeline, the pressure of the media, the temperature, and any cyclic or vibrational behavior of the joint (Bond and Li, 2020). There are numerous types of gaskets, which can be classified into three categories: 1- metallic, 2- non-metallic, 3- semi-metallic (Shorts, 2017).

Kain (1998) have studied the effect of gasket material on the crevice corrosion of a 316 SS flange in seawater, and, according to Table 6, it was reported that carbon fiber, aramid fiber, PTFE, glass-filled PTFE, and graphite/SS gaskets caused severe crevice corrosion. However, the reason for such behavior was not discussed in this work. Indeed, corrosion was only evaluated visually and quantified by measuring the corroded surfaces depth.

Turnbull (1998; 1999) stated that the use of a graphite gasket, which

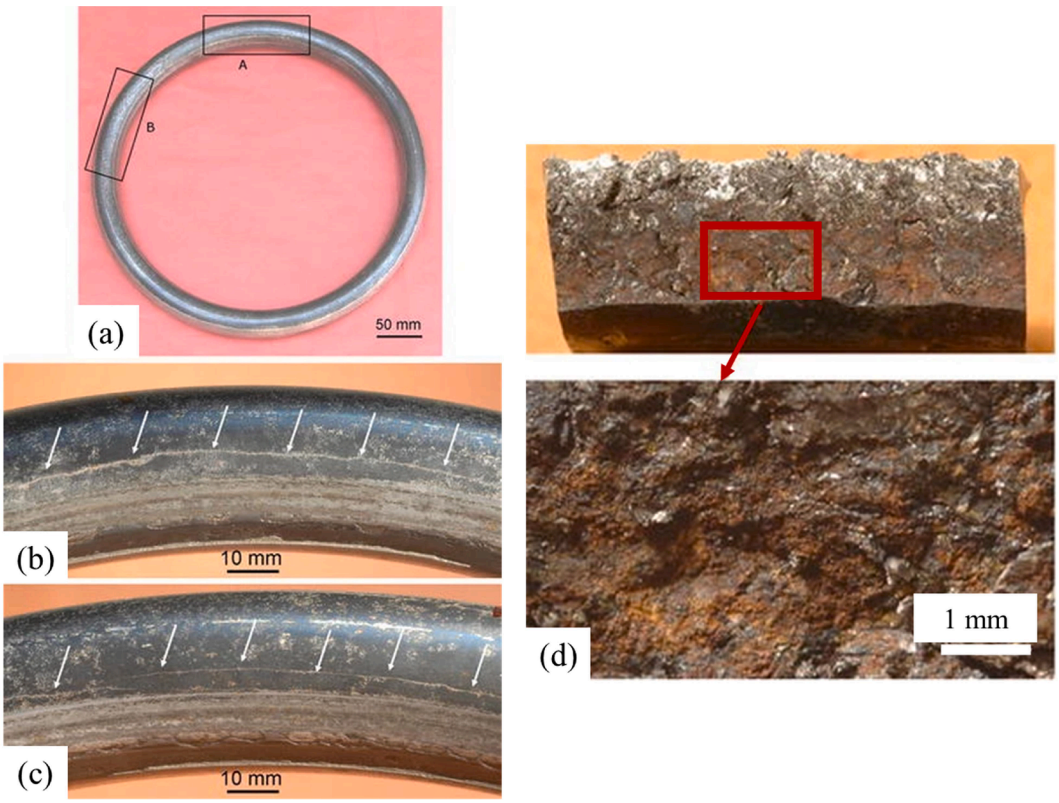

Fig. 15. Ring gasket: (a) overall view of the failed gasket; (b) and (c) close-up views of regions A and B, which reveal cracks; (d) fracture surface of the ring gasket displaying a thick layer of oxides and/or corrosion products[10] (adapted from Gore et al., 2014).

is more noble than DSS, results in an increase in pH within the crevice, thereby preventing crevice corrosion. Flexible graphite gasket is frequently chosen as a sealing material because it offers extensive chemical resistance, a broad temperature range, affordability, outstanding sealing performance, and the ability to provide fire safety. This noble gasket has a higher corrosion potential than the DSS in their used 0.6 M NaCl solution, hence the reaction on the graphite will be net cathodic, and indeed the hydrogen ions (H^+) will be reduced in the crevice. This result is contradictory to Kain (1998) findings, which concluded that graphite gaskets caused severe crevice corrosion. Turnbull's studies indicate that the corrosion potential of graphite in acidic solutions is expected to be more noble than that of DSS in seawater when biofilm formation occurs. Consequently, graphite will act as a cathode within the crevice of this system. This suggests that coupling DSS with a graphite gasket has the potential to mitigate the pH decline within the crevice. Thus, graphite gaskets could help prevent the initiation of crevice corrosion in systems where acidification of the crevice solution serves as a precursor to crevice attack. Turnbull's experiments confirmed this concept by demonstrating that significant acidification within the crevice can be prevented for potentials up to approximately 0.4 V_{SCE}. However, in Kein's experiments, where the applied potential was 0.6 V_{SCE}, the reactions on the graphite surface become net anodic, potentially contributing to the initiation of crevice attack

Rogne et al. (ASTM A182 /A182M - 20 2020) also studied the impact of gasket material on CCT. Tests were carried out by PTFE and rubber bonded aramid gaskets. The CCT of the setup using a PTFE gasket was measured to be 35 °C, whereas the CCT of the setup using an aramid gasket was 42 °C. This indicates that the aramid gasket enhanced the resistance to crevice corrosion. This study uncovered that the porous structure of aramid gaskets facilitated the absorption of seawater, thereby providing the necessary oxygen for the cathodic reaction within the crevice formed between the gasket and flange. Consequently, the acidification of the crevice and the subsequent crevice corrosion were delayed. However, there exists a contradiction between the findings of Rogne and Kain. According to Kain's results (Table 6), aramid fiber gaskets actually accelerated crevice corrosion of the flange. In contrast, Rogne's work identified aramid as a suitable gasket material capable of preventing corrosion. Hence, it appears that other factors, such as the material composition of the flange, may influence the corrosion propagation. Furthermore, discrepancies in the behavior of 316 SS and weld overlays with Ni-based alloys in seawater could contribute to the divergent outcomes observed in these studies.

Martin et al. (2004) determined the sensitivity of several Ni-Cr-Mo alloys to crevice corrosion in seawater at 65 °C and at 0.3 V_{SCE}. Their results showed that fluoroelastomeric gaskets enhanced the resistance of alloys to crevice corrosion, even at higher potentials (0.6 V_{SCE}) and longer exposure times (60 h). X-ray diffraction (XRD), energy-dispersive X-ray spectroscopy (EDX), and Fourier transform infrared spectroscopy (FT-IR) analysis of gasket material and residues on metals revealed that a layer of tac deposited on the surface of the metal prevents the metal from corroding. The tac-related layer originates from the mold release agent used to process fluoroelastomeric gaskets. In agreement with Kein's results (Table 6), this research claims that fluoroelastomeric gaskets could be suitable for sealing.

Literature mainly discusses low-pressure applications for corrosion studies. However, in industrial applications with higher pressures, typically ranging from 65 to 100 bars, metal gaskets or spirally wound gaskets are used due to the risk of blowout in sheet gaskets (Bouzid and Das, 2023). The material of these gaskets should be compatible with the flange material to reduce the risk of galvanic corrosion in seawater

[10] Used with permission of Springer Nature BV, from Stress Corrosion Cracking of Ring Type Joint of Reactor Pipeline of a Hydrocracker Unit, Gore, P., Sujata, M. & Bhaumik, S.K, Volume 14, 2014; permission conveyed through Copyright Clearance Center, Inc.

Table 7
Details of the corrosion failures due to inappropriate gasket material or design.

Type of gasket	Gasket material	Medium	Location of corrosion	Root cause	Mitigation method	Ref.
Spiral wound	DSS 2205 windings, graphite filler	Seawater	Crevice corrosion on the flange face	Gasket material	Using polymeric gaskets instead of spiral wound	(Mathiesen and Bang, 2011)
Sheet	Graphite, and PTFE	Seawater	Crevice corrosion on the flange face	Gasket material	Using elastomer-type gaskets instead of graphite and PTFE gaskets	(Kain, 1998)
Spiral wound	316 L SS inner ring, carbon steel outer ring, 316 L SS hoop, expanded graphite filler	Marine humidity	Flange surface on the contact area with gasket	Water ingress in tightened flanges in modular construction	- Rust preventive coating - Special spiral wound gasket made by vermiculite instead of expanded graphite filler	(Tsuda et al., 2021)
Spiral wound	Monel windings, PTFE filler, and carbon steel ring	Hydrofluoric acid	Flange face	Gasket design	Designed a new customized gasket that prevents the direct contact of the process with the flange face	(Simonton and Barry, 2006a; 2006b)
Sheet	Graphite	Seawater	Crevice corrosion on the flange face	Gasket material	Using non-graphite gasket	(Francis, 1994)
Spiral wound	Carbon steel outer ring	–	Severe corrosion on the outer ring	–	Field tests and risk assessment provided confidence that it was acceptable to continue operation	(Hamblin and Finch, 2001)

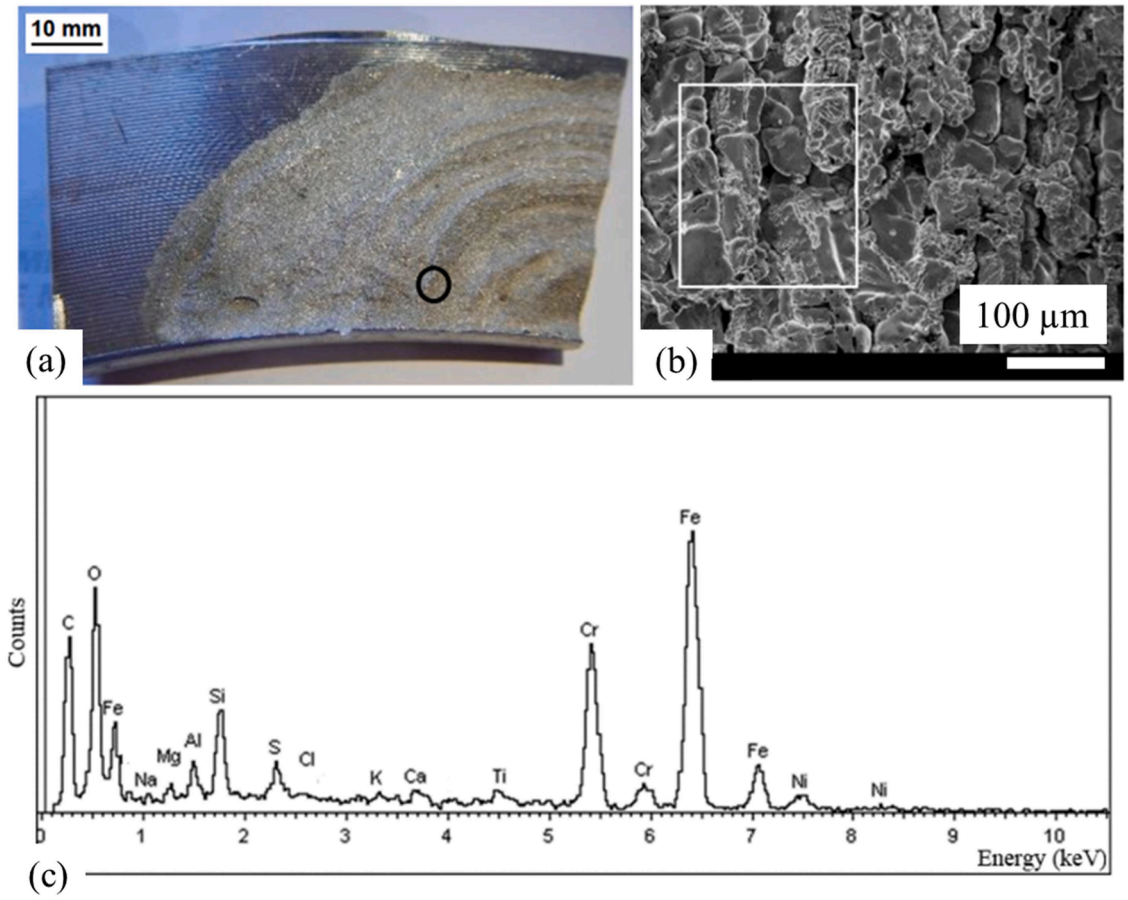

Fig. 16. Analysis of the corroded flange face: (a) the selected region of the corroded surface for SEM analysis; (b) SEM image of the circled region; (c) EDS analysis[11] (adapted from Kölblinger et al., 2022).

(Francis and Byrne, 2007). Mathiesen and Bang (2011) compared crevice corrosion initiation and propagation in a UNS S31254 flange using graphite gaskets, spiral wound gaskets, and polymer gaskets. The results of the polarization tests revealed that the initiation potential for the graphite gasket was lower than for the others, and, in addition, crevice corrosion propagated after initiation with the graphite gasket, while causing repassivation in the cases of polymer and spiral wound gaskets. Stress corrosion cracking (SCC) in a ring type joint (RTJ) caused failure of reactor pipeline of a hydrocracker unit; the ring gasket was made of 347 SS. Examinations showed that the ring gasket had developed a number of discrete cracks as shown in Fig. 15(a), (b), and(c). Fig. 15(d) depicts the corrosion products firmly adhering to the fracture surfaces (Gore et al., 2014). Simonton and Barry (2006a; 2006b) embarked on the development of an innovative gasket design that

[11] Reprinted from Engineering Failure Analysis, Volume 134, A.P. Kölblinger, S.S.M. Tavares, C.A. Della Rovere, A.R. Pimenta, Failure analysis of a flange of superduplex stainless steel by preferential corrosion of ferrite phase, 2022, with permission from Elsevier.

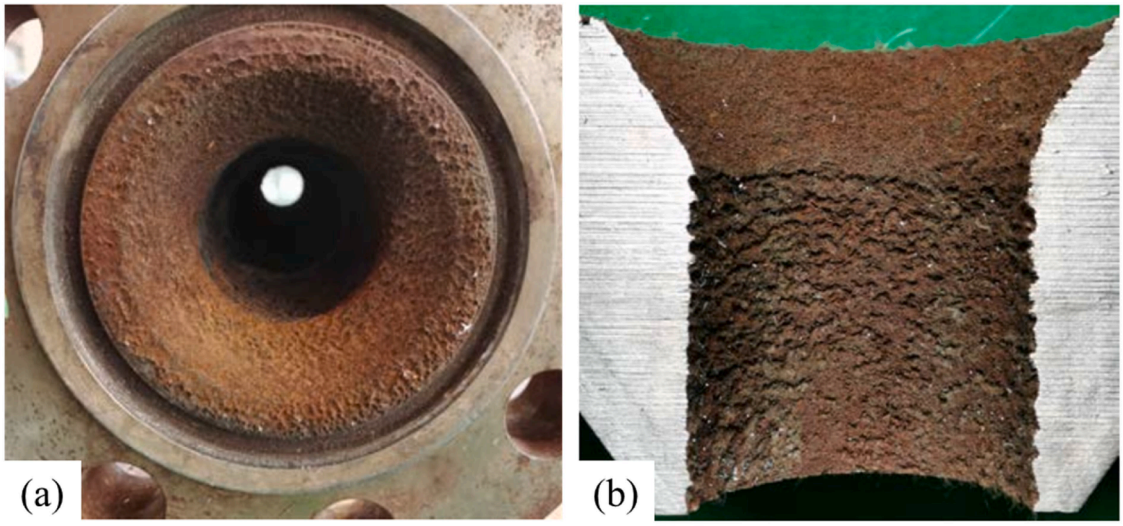

Fig. 17. Macroscopic image of the corroded ASTM A105 flange; (a) corroded sealing groove and inner wall; (b) cross section of the corroded flange[12] (Ji et al., 2023).

distinct from the traditional spiral wound gasket, which typically consists of Monel windings, PTFE filler, and an outer carbon steel ring. Their primary objective was to address a range of critical concerns, which encompassed reducing flange face corrosion, improving handling limitations, and enhancing sealing performance. The researchers observed that the standard spiral wound gasket configuration with a Monel inner ring proved ineffective in preventing corrosion across the entire flange face. They modified the design by adding machined serrations to the ring faces, similar to the kammprofile or serrated metal gasket type. The final design features Monel windings, flexible graphite as the filler material, and a serrated inner ring coated with PTFE. Hamblin and Finch (2001) reported severe corrosion on the outer rings of spiral wound gaskets made from carbon steel, resulting in corrosion-induced removal of the outer ring, which poses a potential risk of diminishing the blowout resistance of the sealing component. Additionally, the expansion of corrosion products had the potential to exert pressure on the flanges, potentially releasing the compressive stress on the sealing element. They stated that replacing the gasket with corrosion-resistant alternatives was not feasible immediately, as it was necessary for the system to remain operational. In addition, implementing individual remedial measures for each flange, such as sealant injection, was also less desirable due to the extensive number of flanges involved. However, after conducting physical testing, theoretical modeling, industrial investigations, and risk assessments, the decision was made to continue the system operation. Table 7 summarizes the details of the corrosion failures due to inappropriate gasket material or design.

Microorganisms

Microbiological species are another factor that may influence corrosion when present in the environment. Corrosion influenced by microbiological activity is known as microbiologically influenced corrosion (MIC). As a result of a microorganism rich environment, pitting and crevice corrosion, selective de-alloying, and differential aeration may occur (Little et al., 2000). Kölblinger et al. (2022) reported the failure of a UNS S32760 SDSS (*PREN* $\geq$ 40) flange, although the chemical composition and microstructure of the material were based on the ASTM A182 standard. Here, in the crevice of the gasket, the flange material suffered preferential corrosion of the ferrite phase. Fig. 16 shows peaks relating to sulfur (S) and chlorine (Cl). In addition to deposits of organic materials that form during stagnant conditions or when there is a low or intermittent liquid flow, resulting in the creation of crevices and differential aeration cells, sulfur is also a characteristic of corrosion induced by microorganisms (i.e., microbiologically influenced corrosion). Furthermore, the service conditions, which involve exposure to 28 °C seawater and the specific geometry and size of the crevice between the gasket and flange, promote the proliferation of bacteria and expedite the corrosion process. In seawater, microorganisms present in water can adhere to surfaces and form biofilms. Biofilms are thin layers of microorganisms that adhere to each other and to surfaces. Mathiesen and Bang (2011) stated that the presence of biofilms in seawater below 40 °C leads to flange material ennoblement, elevating the potential of UNS S31254 to 350 to 450 $mV_{Ag/AgCl}$. This elevation contributes to the initiation and propagation of crevice corrosion, especially when graphite is used in spiral wound gaskets.

Temperature

Larché et al. (2016), revealed that the temperature affects the electrochemical potentials and kinetics of the corrosion initiation and propagation. This work studies the effect of temperature on six types of flanges, including UNS S32205, S32750, N08367, S31266, N06625, and N06022, for three months in both natural and chlorinated seawater. In the seawater solutions at 30 °C, only the surface of the less alloyed S32205 was corroded, but in the solution at 50 °C, corrosion was observed on the surfaces of N08367, S32750, and N06625 flanges. Upon visual examination of the corrosion results, it was observed that the corrosion on the surface of the UNS S32750 flanges was notably severe. In contrast, the propagation of crevice corrosion on the UNS N06625 flanges was relatively limited. Remarkably, the surfaces of the UNS S31266 and UNS N06022 flanges exhibited resistance to crevice corrosion even after three months of exposure to chlorinated seawater at 50 °C.

Rogne et al. (1998) specified CCT for weld overlays of different Ni alloys by increasing the temperature in steps of 5 °C from 20 °C to 100 °C. It was found that the more resistant the alloy, the higher the CCT temperature. In addition, at higher temperatures, the time of corrosion initiation diminished drastically.

[12] Reprinted from Journal of Physics: Conference Series, Nan Ji, Changliang Li, Peng Wang, Lijuan Zhu, and Chun Feng, Corrosion Cause Analysis of a Surface Pipeline Flange, 2023, CC BY 3.0.

Chloride concentration

Chloride concentration is another major influential factor in the crevice corrosion behavior of SSs. Hydrolysis occurs in chlorinated solutions in crevices, causing an increased concentration of acid and chloride in occluded volumes, ultimately resulting in passive film breakdown (Oldfield and Sutton, 1978a; 1978b). An increment in chloride concentration decreases the corrosion resistivity of SSs to localized corrosion. This factor affects the passivity breakdown potential and makes the SS vulnerable to localized corrosion (Ibrahim et al., 2009; Dastgerdi et al., 2019). Tawancy (2019) reported a leakage failure of a 304 SS gasket used as a seal in bolted flanged joints of a hydrocarbon transfer pipeline in a polyethylene plant, as well as in a piping system employed for demineralized water distribution in a polypropylene plant. Root cause analysis indicated that contamination of the water by chloride ions, and excessive compressive preload were the main reasons for the leakage. In some cases, chlorination is carried out in seawater systems to avoid the formation of marine biofilms on the surface of the metal (Mathiesen and Bang, 2011). Larché et al. (2016) reported an open circuit potential (OCP) difference of SS materials in chlorinated and non-chlorinated seawater of about 300 mV. Still, for Ni-based alloys, the increment of OCP in chlorinated seawater was less than 100 mV. This clearly demonstrates that the effect of chlorination is more pronounced in SSs compared to Ni-based alloys. Generally, it has been observed that an increase in chloride concentration in the bulk solution leads to a decrease in the crevice initiation potential for Ni-based alloys (Odahara et al., 2020).

Flow

The effect of fluid flow velocity on the corrosion between gaskets and flanges is considered by the study of Mameri et al. (2000). Their study results showed that increasing the fluid velocity from 1.4 cm s^{-1} to 4.5 cm s^{-1} slightly increased the corrosion rate of carbon steel XC38. Based on this work, it can be hypothesized that the main cathodic reaction is the reduction of oxygen, which is diffusion controlled. Therefore, by increasing the flow rate, the amount of oxygen on the surface of the cathode can be increased, and as a result, the corrosion rate will then rise. Additionally, flow conditions can influence corrosion by either conveying corrosive substances toward the metal surface or carrying away corrosion products from the metal surface. Ji et al. (2023) examined the impact of flow velocity on the corrosion of the inner wall of an ASTM A105 carbon steel flange after one year of service. Fig. 17(a) and (b) demonstrate visible fluid erosion marks on the inner wall surface. Based on their analysis, it was determined that the average flow velocity of the fluid within the pipeline surpassed the critical erosion velocity. Consequently, the fluid flow inside the pipeline caused erosion to the inner wall of the flange. In seawater applications, CRAs often experience heightened corrosion aggressiveness during shutdown periods, leading to stagnant seawater in contact with the flange surface. Seawater stagnation can easily give rise to the formation of differential aeration cells and/or deposits, ultimately compromising the passivity and causing a dramatic propagation of localized corrosion (Larché and Dézerville, 2012).

Corrosion monitoring techniques

Corrosion monitoring and detection methods can be categorized into two groups: offline detection and online monitoring. Offline detection suffers from extended testing cycles and the inability to conduct continuous assessments (Hussein Khalaf et al., 2024). Online corrosion monitoring techniques are valuable for detecting and assessing corrosion in various forms, including localized corrosion. However, traditional corrosion monitoring methods face specific challenges and limitations that can complicate the detection of localized corrosion. Various methods have been introduced in the literature for monitoring pitting corrosion (Orlikowski et al., 2017). However, only a few publications have discussed the monitoring of crevice corrosion (Schmitt et al., 2004; Sun and Yang, 2006). Given the similarity between pitting corrosion and crevice corrosion, and considering that crevice corrosion often initiates with the formation of pits in the occluded regions (Costa et al., 2023), the advantages and disadvantages of monitoring methods for pitting corrosion are also applicable to crevice corrosion. Non-destructive testing methods find extensive use in industrial settings, with the ultrasonic technique (UT) being particularly notable for its ability to observe the dimensions and configurations of pits. Regrettably, this method exhibits low sensitivity, limiting its efficacy to detecting only advanced stages of pitting corrosion. The localized nature of damage necessitates a considerable number of measurements for precise diagnosis (Sun et al., 2009). Another prevalent technique for monitoring pitting corrosion is the acoustic emission method, where acoustic signals are produced by the evolution of hydrogen bubbles or the cracking of passive layers. This method key advantage lies in its capability to capture the early stages of pitting corrosion, attributed to the degradation process of passive layers. Optimal outcomes are achieved for materials featuring thick passive layers, such as aluminum and magnesium alloys (Orlikowski and Darowicki, 2011). Despite its numerous advantages, the acoustic emission method is seldom integrated into online corrosion monitoring systems due to its heightened sensitivity to external noise, a common occurrence in industrial environments (Xu et al., 2011; Mazille et al., 1995). Corrosion monitoring through electrochemical techniques is not without drawbacks and limitations, primarily tied to the generation of corrosion products and variations in the conductivity of the corrosion medium, which can impact measurement accuracy (Cox and Lyon, 1994). Moreover, employing electrochemical methods in the investigation of metal corrosion may distort the actual corrosion reactions of the samples under study due to the necessity for additional interference. Additionally, these methods fall short in precisely identifying localized corrosion or effectively assessing cumulative corrosion processes, as they can only deliver average electrochemical data for a specific region at a specified time (Arellano-Pérez et al., 2018).The most commonly used electrochemical techniques for corrosion monitoring include the corrosion coupon technique, electrochemical resistance probes (ER), linear polarization resistance (LPR), electrochemical impedance spectroscopy (EIS), and electrochemical noise (EN). Various electrochemical techniques for corrosion monitoring are compared in Table 8 (Ma et al., 2019). Artificial intelligence (AI) has recently been used in the field of corrosion monitoring, enhancing precision, speed, and efficacy in the detection and protection against corrosion (Pourrahimi et al., 2023). It is important to remember, nevertheless, that effective data processing and analysis skills are required for the successful application of these strategies, as are dependable communication technologies for sending data from remote locations. (Hussein Khalaf et al., 2024).

Table 8
Comparison of electrochemical techniques for corrosion monitoring (Ma et al., 2019).

Method	ER	LPR	EIS	EN	Coupon
Quantitative localized corrosion	×	×	–	×	✓
Qualitative localized corrosion	×	×	–	✓	✓
General corrosion	✓	✓	✓	✓	✓
Field monitoring use	✓	✓	✓	✓	✓
Response time	2 h to days	Instant	Instant	Instant	10–365 days

Analysis of the flange face corrosion

Gaps or crevices between flanges due to the presence of the gasket are potential places for crevice corrosion to take place. Fig. 18 indicates

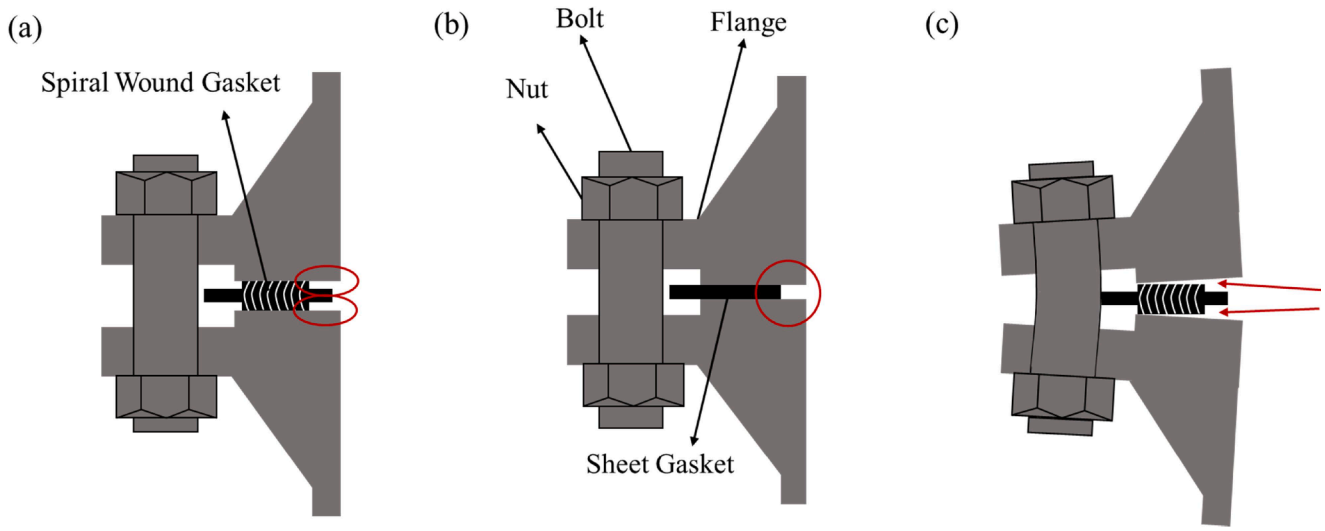

Fig. 18. Schematic of vulnerable places for crevice corrosion between gaskets and flanges: (a) standard spiral wound with inner ring-crevice at ID; (b) standard cut-sheet gasket-crevice at ID; (c) crevices above and below spiral wound inner ring (Worden, 2014).

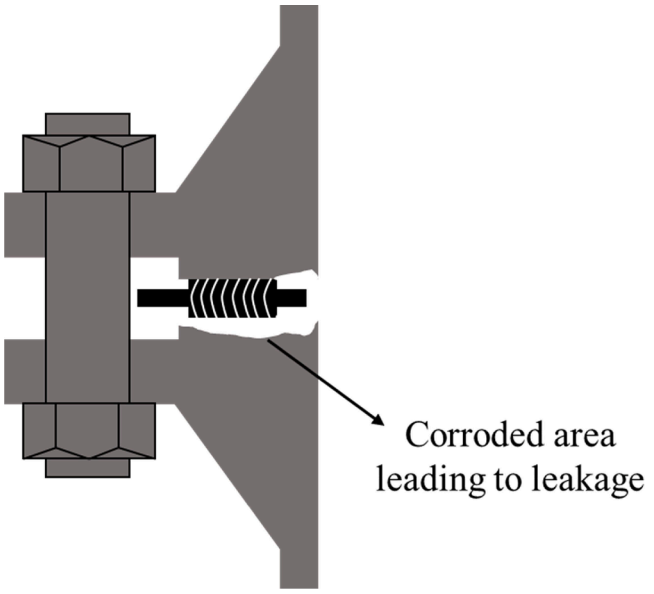

Fig. 19. Schematic illustration depicting crevice corrosion on the flange face at the interface between the flange and the standard spiral wound gasket, resulting in leakage (Worden, 2014).

potential locations for crevice corrosion when using spiral wound and sheet gaskets. There is a gap between the inner ring and the pipe bore Fig. 18(a) and (b)), and the upper and lower zones of the inner ring of spiral wound gaskets which are susceptible to crevice corrosion (Fig. 18 (a)) (Worden, 2014). Fig. 18(c) illustrates the distribution of bolt load along the outer diameter (OD) of the flange, resulting in bending around the bolt circle and causing the flange to lift off from the inner diameter (ID) of the gasket. This phenomenon creates potential gaps that can facilitate the occurrence of crevice corrosion. The zones described with a circle in the flange face near the gasket inside diameter are crevices containing small amounts of stagnant fluid. A high rate of metal dissolution occurs in these crevice regions according to the mechanism discussed in the crevice corrosion section. After a period of time, enough mass loss occurs enlarging the crevice zone toward the outside causing failure by creating a leak path in the flange facing (as shown in Fig. 19). Creep in bolted flanged joints is a phenomenon where the bolts and the flange components deform over time due to the influence of mechanical

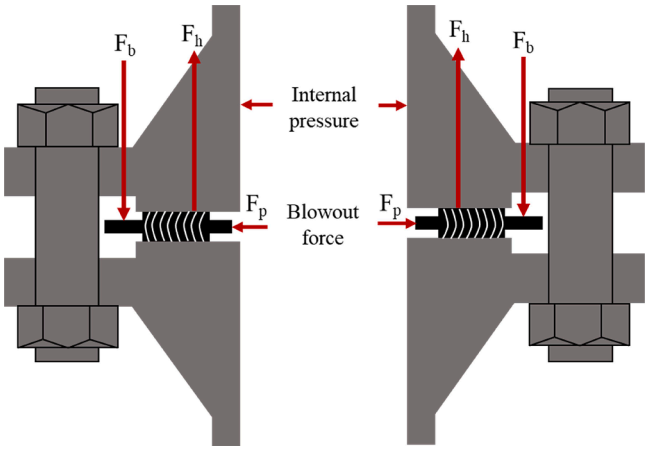

Fig. 20. Illustrative diagram depicting the mechanical forces applied on the gasket in action. The red arrows identify each force, including the compressive force generated by tightening the bolts (F_b), the hydrostatic force (F_h), and the blow out force (F_p).

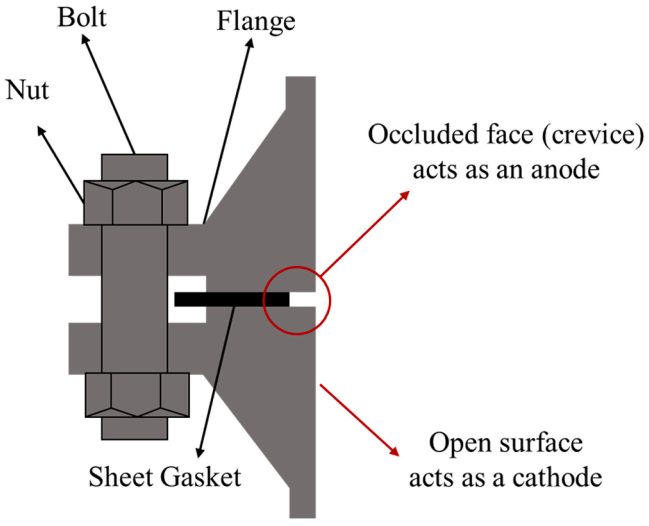

Fig. 21. Illustration of crevice corrosion in bolted flanged gasketed joints, highlighting the anode and cathode regions.

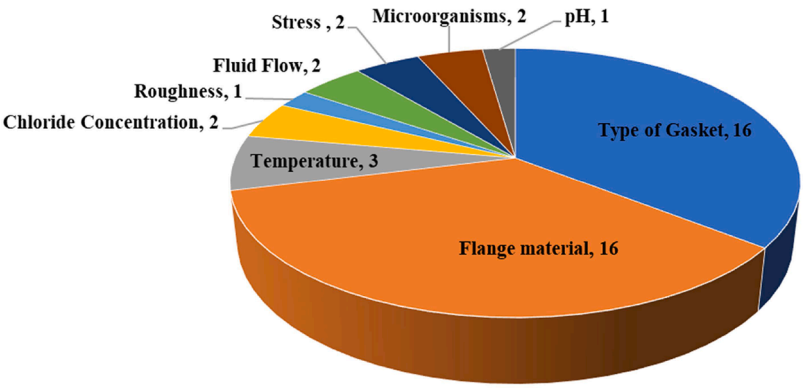

Fig. 22. Studied factors in papers examined flange corrosion in bolted flanged joints.

loads and elevated temperatures (Sawa et al., 2015; Kanthabhabha et al., 2020). The deformation caused by the gasket and bolt creep can result in the formation of crevices or gaps at the flange facings (Efremov, 2005).

Corrosion on the flange surface or gasket can result in surface irregularities and inadequate compression force, thereby increasing the risk of leakage. In Fig. 20, the diagram illustrates the forces acting on gaskets in a bolted flanged joint (Tawancy, 2019). Prior to pressurizing the system, the gasket experiences a compressive force (F_b) generated by tightening the bolts, effectively compressing the gasket into the flange to establish a seal and prevent fluid leakage between the flanges. Once the system is pressurized, opposing forces come into play: the hydrostatic force (F_h), which seeks to separate the flanges, and the blowout force (F_p), which aims to displace the gasket. To counteract the combined impact of the hydrostatic force and the blowout force, additional bolt tightening is required to maintain the gasket in position. However, excessive compression force, beyond what is necessary to counteract these opposing forces, may eventually lead to gasket deformation. Furthermore, non-uniform preload can introduce localized variations in gasket stresses. Taking these forces into consideration, the corrosion process can intensify the hydrostatic and blowout forces, leading to the unloading of the preload and, ultimately, causing leakage. As per the literature, corrosion affecting the outer ring of the spiral wound gasket (made of carbon steel) can diminish the gasket resistance to blowout forces. Furthermore, the corrosion of carbon steel flange faces may induce the expansion of corrosion products, potentially opening the flanges apart and relieving the compressive stress on the sealing element, ultimately resulting in leakage (Hamblin and Finch, 2001).

As shown in Fig. 21, in flanged joints, there are two surfaces: the occluded face, which is the surface facing the gasketed joint, and the open surface. The occluded face typically acts as an anode for those alloys that are passive, while the open surface acts as a cathode, except in cases where the gasket is a nobler material (e.g., graphite). The extent of oxidant presence and its accessibility to the open flange surface are critical factors influencing the anodic dissolution reaction within the crevice, ultimately leading to an increased rate of crevice corrosion. What makes crevice corrosion notably challenging is the contrasting availability of oxygen, or other oxidants. Oxygen is often more abundant on the open flange surface, where it can facilitate the formation of a protective oxide layer.

Discussion

The distribution and fraction of the studied factors in the field of corrosion phenomena in bolted flanged systems are presented in Fig. 22 to better understand the most important failure factors and the factors that are understudied in the literature. Most of these studies investigated the material of the flange and the type of gasket. As well, it can be concluded that SSs and nickel-based alloys dominated the studied flange materials in most cases. It was reported that the *PREN* value could be used to compare corrosion resistance of flange materials to pitting and crevice corrosion, with higher values of *PREN* indicating greater resistance. However, environmental factors and specific microstructures resulted in corrosion failure of alloys with a high *PREN*. Temperature, chloride concentration, roughness, fluid flow, stress, microorganisms, and pH are all factors that may influence flange corrosion, but very few studies have addressed them. The primary function of a gasket is to provide a leak-tight seal and to provide electrical insulation at the same time. Most of the gaskets used for critical services are semi metallic, such as spiral wound gaskets, Kammprofiles, etc. While these products can provide leak-tight seals when well designed, their metallic nature allows electrons flow between flanges, which may induce galvanic corrosion. Graphite gaskets are commonly considered inappropriate for use in seawater systems because the noble galvanic properties of the material lead to accelerated corrosion of the anodic flange material. However, such gaskets are useful for systems that operate at high temperatures.

There is a substantial amount of research on crevice and galvanic corrosion, which are among the main corrosion mechanisms on the flange surface, however, the majority of these studies are solely focused on experiments carried out by conditions which are not close to industrial applications. In these documented experiments, the assessment of materials occurs under conditions that deviate from those commonly encountered in industrial applications. For instance, these experiments neglect factors such as crevice geometry, the presence of fluid flow, and gasket contact stress. None of the studied papers and existing standards (e.g., ASTM, ISO) have proposed a scientific approach to analyze and predict the corrosion behavior of the flange in the presence of specific service conditions and different gasket materials.

Conclusion

This review study documents failures in bolted flanged gasketed joints due to flange face corrosion and discusses the influence of the crucial factors on degradation by corrosion in these cases.

- Corrosion may occur on the inner side of the flange and the flange surface between gaskets and flanges. The gaps or crevices between gaskets and flanges are potential places for crevice corrosion which can be accelerated by the significant potential difference between the gasket and flange material, i.e., galvanic corrosion, sensitization due to welding on the flange surface, and the presence of deleterious phases in the flange material.
- Based on the conducted literature review, it was concluded that most studies reveal that the flange and gasket materials are the most problematic factors for flange face corrosion. Only a few studies discuss the influence of environmental factors, such as temperature, chlorination, and flow on corrosion behavior of bolted flanged systems.

- Indeed, the majority of the reviewed literature focused on investigating the consequences of corrosion following the occurrence of failure, while limited attention was given to preventive analysis of such failures or corrosion monitoring systems in this specific case. As a result, it can be inferred that there is currently a lack of studies that examine the factors influencing corrosion phenomena in bolted flanged joints and that provide predictions regarding the corrosion behavior of flanges prior to failure.
- Most corrosion mitigation methods identified in the literature focus on flange and gasket material selection or altering gasket design. The literature reveals a limited number of studies proposing the implementation of coating and cathodic protection methods for corrosion prevention.
- Emerging AI techniques might be promising in the field of corrosion monitoring for flanged gasketed joints, and there is a gap in research within this field, highlighting the need for further exploration and investigation.

CRediT authorship contribution statement

Soroosh Hakimian: Writing – original draft, Methodology, Investigation, Formal analysis, Conceptualization. **Abdel-Hakim Bouzid:** Writing – review & editing, Supervision, Methodology, Funding acquisition. **Lucas A. Hof:** Writing – review & editing, Supervision, Methodology, Conceptualization, Funding acquisition.

Declaration of competing interest

The authors declare that they have no known competing financial interests or personal relationships that could have appeared to influence the work reported in this paper.

Data availability

No data was used for the research described in the article.

Acknowledgment

This work was supported by the Natural Sciences and Engineering Research Council of Canada (NSERC) under the Discovery Grant (RGPIN-2019-05973 and RGPIN-2021-03780).

References

ASTM G150-18 Standard Test Method for Electrochemical Critical Pitting Temperature Testing of Stainless Steels and Related Alloys. West Conshohocken, PA: 2018.

Abid, M., Nash, D.H., 2003. Comparative study of the behaviour of conventional gasketed and compact non-gasketed flanged pipe joints under bolt up and operating conditions. Int. J. Press. Vessel. Pip. 80, 831–841. https://doi.org/10.1016/J.IJPVP.2003.11.013.

Al-Abbadi, S., Aoudi, H., AlShouly, W., Saeed, W., AlSafatli, K., Toubar, A., 2017. Crevice corrosion effect on alloy 625 in untreated seawater environment. In: Society of Petroleum Engineers - SPE Abu Dhabi International Petroleum Exhibition and Conference 2017. https://doi.org/10.2118/188302-MS.

Arellano-Pérez, J.H., Ramos Negrón, O.J., Escobar-Jiménez, R.F., Gómez-Aguilar, J.F., Uruchurtu-Chavarín, J, 2018. Development of a portable device for measuring the corrosion rates of metals based on electrochemical noise signals. Measurement 122, 73–81. https://doi.org/10.1016/j.measurement.2018.03.008.

ASTM A105 /A105M - 18 Standard specification for carbon steel forgings for piping applications n.d. https://www.astm.org/Standards/A105 (accessed November 30, 2020).

ASTM A182 /A182M - 20 Standard specification for forged or rolled alloy and stainless steel pipe flanges, forged fittings, and valves and parts for high-temperature service n.d. https://www.astm.org/Standards/A182.htm (accessed November 30, 2020).

ASTM A350 /A350M - 18 Standard specification for carbon and low-alloy steel forgings, requiring notch toughness testing for piping components n.d. https://www.astm.org/Standards/A350.htm (accessed November 30, 2020).

ASTM G192-08(2020)e1 Standard Test Method For Determining the Crevice Repassivation Potential of Corrosion-Resistant Alloys Using a Potentiodynamic-Galvanostatic-Potentiostatic Technique. West Conshohocken, PA: 2020.

ASTM G48-11(2020)e1, Standard Test Methods For Pitting and Crevice Corrosion Resistance of Stainless Steels and Related Alloys By Use of Ferric Chloride Solution. West Conshohocken: 2020.

ASTM G61 - 86(2018) Standard test method for conducting cyclic potentiodynamic polarization measurements for localized corrosion susceptibility of iron-, nickel-, or cobalt-based alloys n.d. https://www.astm.org/Standards/G61.htm (accessed October 28, 2021).

ASTM G71-81(2019)- Standard Guide for Conducting and Evaluating Galvanic Corrosion Tests in Electrolytes. West Conshohocken, PA: 2019.

ASTM G78 - 20 Standard guide for crevice corrosion testing of iron-base and nickel-base stainless alloys in seawater and other chloride-containing aqueous environments n.d. https://www.astm.org/Standards/G78.htm (accessed November 9, 2021).

Bengtsson M. Investigation of galvanic corrosion between graphite gaskets and stainless steel flanges. 2015.

Betts, A.J., Boulton, L.H., 1993. Crevice corrosion: review of mechanisms, modelling, and mitigation. Br. Corros. J. 28, 279–296.

Bond, S., Lattimer, A., Welsford, P., 2018. Flange face corrosion in seawater and hydrocarbon environments related to gasket material selection. Corros. Prevent. 2018.

Bond, S., Li, Yi, 2020. A novel gasket design for an isolating gasket to solve common sealing problems. Corrosion 2020.

Bouzid, A., Chaaban, A., Bazergui, A., 1994. The influence of the flange rotation on the leakage performance of bolted flanged joints. Canad. Soc. Mech. Eng.

Bouzid, A., Chaaban, A., Bazergui, A., 1995. The effect of gasket creep-relaxation on the leakage tightness of bolted flanged joints. J. Press. Vessel. Technol. 117, 71–78. https://doi.org/10.1115/1.2842093.

Bouzid, A.-H., Das, S.K., 2023. Long-term performance of semimetallic gaskets. J. Nucl. Eng. Radiat. Sci. 9 https://doi.org/10.1115/1.4056260.

Bouzid, A.H., 2009. On the effect of external bending loads in bolted flange joints. J. Press. Vessel. Technol. 131 https://doi.org/10.1115/1.3006895/474944. Transactions of the ASME.

Bouzid, A.H., Derenne, M., El-Rich, M., Birembaut, Y., 2004. Effect of flange rotation and gasket width on the leakage behavior of bolted flanged joints. Weld. Res. Council Bull.

Bradford, S.A., 2003. Corrosion. Encyclopedia of Physical Science and Technology, 3rd Edition, pp. 761–778. https://doi.org/10.1016/B0-12-227410-5/00148-4.

Brondel, D., Edwards, R., Hayman, A., Hill, D., Mehta, S., Semerad, T., 1994. Corrosion in the oil industry. Oilfield Rev. 6, 4–18.

Costa, E.M., Dedavid, B.A., Santos, C.A., Lopes, N.F., Fraccaro, C., Pagartanidis, T., et al., 2023. Crevice corrosion on stainless steels in oil and gas industry: a review of techniques for evaluation, critical environmental factors and dissolved oxygen. Eng. Fail. Anal. 144, 106955 https://doi.org/10.1016/J.ENGFAILANAL.2022.106955.

Cox, A., Lyon, S.B., 1994. An electrochemical study of the atmospheric corrosion of mild steel-I. Experimental method. Corros. Sci. 36, 1167–1176. https://doi.org/10.1016/0010-938X(94)90141-4.

Dastgerdi, A.A., Brenna, A., Ormellese, M., Pedeferri, M.P., Bolzoni, F., 2019. Experimental design to study the influence of temperature, pH, and chloride concentration on the pitting and crevice corrosion of UNS S30403 stainless steel. Corros. Sci. 159 https://doi.org/10.1016/j.corsci.2019.108160.

Efremov, A.I., 2005. In: Creep limitation of bolted fasteners and gaskets. 2005 ASME Pressure Vessels and Piping Conference, PVP2005, July 17, 2005 - July 21, 2005, vol. 3, Denver, CO, United States: American Society of Mechanical Engineers, pp. 167–171. https://doi.org/10.1115/PVP2005-71130.

Esmailzadeh, S., Aliofkhazraei, M., Sarlak, H., 2018. Interpretation of cyclic potentiodynamic polarization test results for study of corrosion behavior of metals: a review. Prot. Metals Phys. Chem. Surfaces 54, 976–989. https://doi.org/10.1134/S207020511805026X.

Martin, Farrel J., Natishan, Paul M., Lawrence, Steven H., Hogan, Elizabeth A., Lucas, Keith E., Thomas, Elvin Dail, 2004. Fluoroelastomeric gasket peculiarities influence the seawater crevice corrosion susceptibility of NiCrMo alloys. Corrosion. New Orleans, Louisiana: 2004.

Fargas, G., Anglada, M., Mateo, A., 2009. Effect of the annealing temperature on the mechanical properties, formability and corrosion resistance of hot-rolled duplex stainless steel. J. Mater. Process. Technol. 209, 1770–1782. https://doi.org/10.1016/j.jmatprotec.2008.04.026.

Fischer, C., Zitter, H., 1960. Korrosion an Dichtflächen von Flanschverbindungen. Mater. Corros. 11, 17–22.

Francis, R., 1994a. Galvanic corrosion of high alloy stainless steels in sea water. Bri. Corros. J. 29, 53–57. https://doi.org/10.1179/000705994798268033.

Francis, R., 1994b. Galvanic corrosion of high alloy stainless steels in sea water. Br. Corros. J. 29, 53–57.

Francis, R., Byrne, G., 2007. Factors affecting gasket selection for stainless steels in seawater. Corrosion 2007.

Gore, P., Sujata, M., Bhaumik, S.K., 2014. Stress corrosion cracking of ring type joint of reactor pipeline of a hydrocracker unit. J. Fail. Anal. Prevent. 14, 307–313. https://doi.org/10.1007/S11668-014-9820-8/TABLES/2.

Guo, D., Chen, J., Chen, X., Shi, Q., Cristino, V.A.M., Kwok, C.T., et al., 2021. Pitting corrosion behavior of friction-surfaced 17-4PH stainless steel coatings with and without subsequent heat treatment. Corros. Sci. 193 https://doi.org/10.1016/j.corsci.2021.109887.

Hack, H.P., 2016. Galvanic corrosion. Reference Mod. Mater. Sci. Mater. Eng. https://doi.org/10.1016/B978-0-12-803581-8.01594-0.

Hakimian, S., Bouzid, A.-H., Hof, L.A., 2023a. An improved fixture to quantify corrosion in bolted flanged gasketed joints. J. Press. Vessel. Technol. 1–27. https://doi.org/10.1115/1.4063975.

Hakimian, S., Hof, L., Bouzid, H.A., 2022. Investigation of corrosion in bolted flanged joints using a novel experimental setup. In: Electrochemical Society Meeting Abstracts 241. The Electrochemical Society, Inc., p. 990

Hakimian, S., Pourrahimi, S., Bouzid, A.-H., Hof, L.A., 2023b. Application of machine learning for the classification of corrosion behavior in different environments for material selection of stainless steels. Comput. Mater. Sci. 228, 112352 https://doi.org/10.1016/J.COMMATSCI.2023.112352.

Hamblin, M., Finch, P., 2001. Dealing with some troublesome flanges. In: 2001 ASME Pressure Vessels and Piping Conference, July 23, 2001 - July 26, 2001, vol. 426, Atlanta, GA, United States: American Society of Mechanical Engineers, pp. 121–129.

Hu, Q., Liu, Y., Zhang, T., Wang, F., 2020. Corrosion failure analysis on the copper alloy flange by experimental and numerical simulation. Eng. Fail. Anal. 109, 104276 https://doi.org/10.1016/J.ENGFAILANAL.2019.104276.

Hu, Q., Zhang, G., Qiu, Y., Guo, X., 2011. The crevice corrosion behaviour of stainless steel in sodium chloride solution. Corros. Sci. 53, 4065–4072. https://doi.org/10.1016/j.corsci.2011.08.012.

Hussein Khalaf, A., Xiao, Y., Xu, N., Wu, B., Li, H., Lin, B., et al., 2024. Emerging AI technologies for corrosion monitoring in oil and gas industry: a comprehensive review. Eng. Fail. Anal. 155, 107735 https://doi.org/10.1016/j.engfailanal.2023.107735.

Ibrahim, M.A.M., Abd El Rehim, S.S., Hamza, M.M, 2009. Corrosion behavior of some austenitic stainless steels in chloride environments. Mater. Chem. Phys. 115, 80–85. https://doi.org/10.1016/J.MATCHEMPHYS.2008.11.016.

Ji, N., Li, C., Wang, P., Zhu, L., Feng, C., 2023. Corrosion cause analysis of a surface pipeline flange. J. Phys. Conf. Ser. 2468, 012171 https://doi.org/10.1088/1742-6596/2468/1/012171.

Kain, R.M., 1998. Gasket materials and other factors influencing the crevice corrosion resistance of stainless steel flanges. Corrosion 98.

Kang, D.H., Lee, H.W., 2013. Study of the correlation between pitting corrosion and the component ratio of the dual phase in duplex stainless steel welds. Corros. Sci. 74, 396–407. https://doi.org/10.1016/j.corsci.2013.04.033.

Kanthabhabha, Jeya RP, Zhao, Z., Bouzid, A.-H, 2020. Creep-relaxation modeling of HDPE and polyvinyl chloride bolted flange joints. J. Press. Vessel. Technol. 142 https://doi.org/10.1115/1.4047211. Transactions of the ASME.

Kazeminia, M., Bouzid, A.-H., 2016. Predicting leakage in packed stuffing boxes. In: 23rd International Conference on Fluid Sealing 2016, March 2, 2016 - March 3, 2016, Manchester, United Kingdom: BHR Group Limited, pp. 45–59.

Kelly, R.G., Lee, J.S., 2018. Localized corrosion: crevice corrosion. Encycl. Interfac. Chem. Surf. Sci. Electrochem. 291–301. https://doi.org/10.1016/B978-0-12-409547-2.13420-1.

Kennell, G.F., Evitts, R.W., Heppner, K.L., 2008. A critical crevice solution and IR drop crevice corrosion model. Corros. Sci. 50, 1716–1725. https://doi.org/10.1016/J.CORSCI.2008.02.020.

Kölblinger, A.P., Tavares, S.S.M., Della Rovere, C.A., Pimenta, A.R, 2022. Failure analysis of a flange of superduplex stainless steel by preferential corrosion of ferrite phase. Eng. Fail. Anal. 134, 106098 https://doi.org/10.1016/J.ENGFAILANAL.2022.106098.

Kruger, J., Begum, S., 2016. Corrosion of metals: overview. Refer. Mod. Mater. Sci. Mater. Eng. https://doi.org/10.1016/B978-0-12-803581-8.02708-9.

Larché, N., Dézerville, P., 2012. Review of material selection and corrosion in seawater reverse osmosis desalination plants. New Pub. Balaban 31, 121–133. https://doi.org/10.5004/DWT.2011.2362.

Larché, Nicolas, Thierry, Dominique, Boillot, Pauline, Cassagne, Thierry, Blanc, Jéréme, Dézerville, Philippe, Johansson, Elisabeth, Lardon, Jean Marc, 2016. Crevice corrosion performance of high grade stainless steels and Ni-based alloys in natural and treated seawater. Corrosion 2016. Vancouver, British Columbia.

Little, B.J., Ray, R.I., Pope, R.K., 2000. Relationship between corrosion and the biological sulfur cycle: a review. Corrosion 56.

Long, Y., Luo, J., Yue, M., Wu, G., Zhao, M., Ji, N., et al., 2022. Investigation on leakage cause of 13Cr pipe flange used for a Christmas tree in a high-pressure and high-temperature gas well. Eng. Fail. Anal. 142, 106793 https://doi.org/10.1016/J.ENGFAILANAL.2022.106793.

Luo, B., Hu, Q., Liu, J., Huang, F., 2022. Effect of crevice gap on crevice corrosion initiation and development of 2205 duplex stainless steel in NaCl solution. J. Mater. Res. Technol. 21, 2584–2597. https://doi.org/10.1016/J.JMRT.2022.10.059.

Ma, C., Wang, Z., Behnamian, Y., Gao, Z., Wu, Z., Qin, Z., et al., 2019. Measuring atmospheric corrosion with electrochemical noise: a review of contemporary methods. Measurement 138, 54–79. https://doi.org/10.1016/j.measurement.2019.02.027.

Mameri, N., Piron, D.L., Bouzid, A., Derenne, M., Marchand, L., Birembaut, Y., 2000. Corrosion quantification test for flanges with graphite-based gaskets. Mater. Perform. 39.

Mathiesen T., Andersen A. Challenges in Pre-Qualification Corrosion Testing of CRAs Based On ASTM G48. NACE Corrosion 2014, San Antonio, TX: 2013.

Troels Mathiesen; Henrik Bang. Accelerated crevice corrosion testing of 6Mo stainless steel flanges with different gasket materials in seawater. EUROCORR 2011, Stockholm: 2011.

Mazille, H., Rothea, R., Tronel, C., 1995. An acoustic emission technique for monitoring pitting corrosion of austenitic stainless steels. Corros. Sci. 37, 1365–1375. https://doi.org/10.1016/0010-938X(95)00036-J.

Nadarajah, C., 2004. A parametric study of ASME B16.5 flanges which has experienced flange face corrosion. In: Proceedings of the ASME/JSME 2004 Pressure Vessels and Piping Conference. Pressure Vessel and Piping Codes and Standards, San Diego, California, USA, pp. 157–163.

Nechache, A., Bouzid, A.H., 2007. Creep analysis of bolted flange joints. Int. J. Press. Vessel. Pip. 84, 185–194. https://doi.org/10.1016/J.IJPVP.2006.06.004.

Nechache, A., Bouzid, A.H., 2008. On the use of plate theory to evaluate the load relaxation in bolted flanged joints subjected to creep. Int. J. Press. Vessel. Pip. 85, 486–497. https://doi.org/10.1016/J.IJPVP.2008.01.005.

Nelson, N.R., Prasad, S., Sekhar, A.S., 2023. Structural integrity and sealing behaviour of bolted flange joint: a state of art review. Int. J. Press. Vessel. Pip. 204, 104975 https://doi.org/10.1016/j.ijpvp.2023.104975.

Nurhadiyanto, D., 2014. Influence of Surface Roughness On Leakage of the Corrugated Metal Gasket. Yamaguchi University.

Odahara, M., Tsuchiya, H., Fujimoto, S., Salgado, D.M., Lillard, S., Lillard, R.S., et al., 2020. Quantifying alloy 625 crevice corrosion using an image differencing technique: part I. initiation and propagation. J. Electrochem. Soc. 167, 021511 https://doi.org/10.1149/1945-7111/AB6EE6.

Okonkwo, B.O., Ming, H., Meng, F., Wang, J., Xu, X., Han, E.-H., 2021. Galvanic corrosion study between low alloy steel A508 and 309/308L stainless steel dissimilar metals: a case study of the effects of oxide film and exposure time. J. Nucl. Mater. 548 https://doi.org/10.1016/j.jnucmat.2021.152853.

Oldfield, J.W., 1987. Test techniques for pitting and crevice corrosion resistance of stainless steels and nickel-base alloys in chloride-containing environments. Int. Mater. Rev. 32, 153–172. https://doi.org/10.1179/095066087790150313.

Oldfield, J.W., Sutton, W.H., 1978a. Crevice corrosion of stainless steels: I. A mathematical model. Br. Corros. J. 13, 13–22. https://doi.org/10.1179/000705978798358671.

Oldfield, J.W., Sutton, W.H., 1978b. Crevice corrosion of stainless steels: II. Experimental studies. Br. Corros. J. 13, 104–111. https://doi.org/10.1179/000705978798276258.

Orlikowski, J., Darowicki, K., 2011. Investigations of pitting corrosion of magnesium by means of DEIS and acoustic emission. Electrochim Acta 56, 7880–7884. https://doi.org/10.1016/j.electacta.2010.12.021.

Orlikowski, J., Jazdzewska, A., Mazur, R., Darowicki, K., 2017. Determination of pitting corrosion stage of stainless steel by galvanodynamic impedance spectroscopy. Electrochim Acta 253, 403–412. https://doi.org/10.1016/j.electacta.2017.09.047.

Pickering, H.W., 1989. The significance of the local electrode potential within pits, crevices and cracks. Corros. Sci. 29, 325–341. https://doi.org/10.1016/0010-938X(89)90039-5.

Pourrahimi, S., Hakimian, S., Bouzid, A.-H., Hof, L.A., 2023. On the use of machine learning algorithms to predict the corrosion behavior of stainless steels in lactic acid. Metals (Basel) 13, 1459. https://doi.org/10.3390/met13081459.

Rice, D.A., Waterland, A.F., 2014. Environmental considerations for gasket selection and the development of an emissions calculator for gasket materials. In: American Society of Mechanical Engineers, 2. Pressure Vessels And Piping Division (Publication) PVP. https://doi.org/10.1115/PVP2014-28024.

Rogne, T., Drugli, J.M., Solem, T., Salbu, H., Skjellevik, H., 1998. Crevice corrosion properties of weld overlays of nibased alloys compared to 6Mo stainless steels for seawater applications. In: Corrosion, 1998- March. NACE International, San Diego, CA, United States.

Sawa, T., Takagi, Y., Torii, H., 2015. Effect of material properties of gasket on the sealing performance of pipe flange connections at elevated temperature. In: ASME 2015 Pressure Vessels and Piping Conference, PVP 2015, July 19, 2015 – July 23, 2015, vol. 2, Boston, MA, United States: American Society of Mechanical Engineers (ASME). https://doi.org/10.1115/PVP2015-45177. Pressure Vessels and Piping Division.

Schmitt, G., Moeller, K., Plagemann, P., 2004. Online monitoring of crevice corrosion with electrochemical noise. Mater. Corros. 55, 742–747. https://doi.org/10.1002/maco.200403812.

Shojaei, E., Mirjalili, M., Moayed, M.H., 2019. The influence of the crevice induced IR drop on polarization measurement of localized corrosion behavior of 316L stainless steel. Corros. Sci. 156, 96–105. https://doi.org/10.1016/J.CORSCI.2019.04.030.

Shorts, M., 2017. Gasket Handbook, 1st ed. Fluid Sealing Association, and European Sealing Association, Wayne, PA.

Simonton, J., Barry, L., 2006a. Evolution of new gasket type increases reliability in HF alkylation unit. In: Proceedings of the ASME 2006 Pressure Vessels and Piping/ICPVT-11 Conference. Volume 7: Operations, Applications, and Components, Vancouver, BC, Canada: ASME, pp. 431–433.

Simonton, J.L., Barry, L.K., 2006b. Evolution of a more reliable gasket for HF alkylation units. Seal. Technol. 12–14. https://doi.org/10.1016/S1350-4789(06)71457-X, 2006.

Sridhar, N., 2022. Localized corrosion in seawater: a bayesian network-based review. Corrosion 79, 268–283. https://doi.org/10.5006/4215.

Sridhar, N., Cragnolino, G.A., 1993. Applicability of repassivation potential for long-term prediction of localized corrosion of alloy 825 and type 316L stainless steel. Corrosion 49.

Standard Specification for Forged or Rolled Nickel Alloy Pipe Flanges, Forged Fittings, and Valves and Parts for Corrosive High-Temperature Service n.d. https://www.astm.org/b0462-18e01.html (accessed April 6, 2022).

Sun, D., Jiang, Y., Tang, Y., Xiang, Q., Zhong, C., Liao, J., et al., 2009. Pitting corrosion behavior of stainless steel in ultrasonic cell. Electrochim Acta 54, 1558–1563. https://doi.org/10.1016/j.electacta.2008.09.056.

Sun X., Yang L. Real-time monitoring of crevice corrosion propagation rates in simulated seawater using coupled multielectrode array sensors 2006.

Tavares, S.S.M., Pardal, J.M., Almeida, B.B., Mendes, M.T., Freire, J.L.F., Vidal, A.C., 2018. Failure of superduplex stainless steel flange due to inadequate microstructure and fabrication process. Eng. Fail. Anal. 84, 1–10. https://doi.org/10.1016/J.ENGFAILANAL.2017.10.007.

Tawancy, H.M., 2019. Failure analysis of 304 stainless steel components used in petrochemical industry applications. Metallogr. Microstruct. Anal. 8, 705–712. https://doi.org/10.1007/s13632-019-00578-5.

Tsuda, Takahiro, Satake, Nozomi, Itoki, Manabu, 2021. Mitigation of flange face corrosion during plant construction. Corrosion 2021. Virtual.
Turnbull, A., 1998. Prevention of crevice corrosion by coupling to more noble materials? Corros. Sci. 40, 843–845. https://doi.org/10.1016/S0010-938X(97)00169-8.
Turnbull, A., 1999. Impact of graphite gasket/duplex stainless steel couples on crevice chemistry and the likelihood of crevice attack in seawater. Corrosion 55.
Westin, E.M., Hertzman, S., 2014. Element distribution in lean duplex stainless steel welds. Weld. World 58, 143–160. https://doi.org/10.1007/s40194-013-0108-5.
Worden, K., 2014. Flange corrosion: prevention and mitigation through better gasketing. In: Fuels and petrochemicals division 2014 - core programming area at the 2014 AIChE spring meeting and 10th global congress on Process Safety, 2, pp. 1000–1008.
Xu, J., Wu, X., Han, E.H., 2011. Acoustic emission during pitting corrosion of 304 stainless steel. Corros. Sci. 53, 1537–1546. https://doi.org/10.1016/J.CORSCI.2011.01.030.